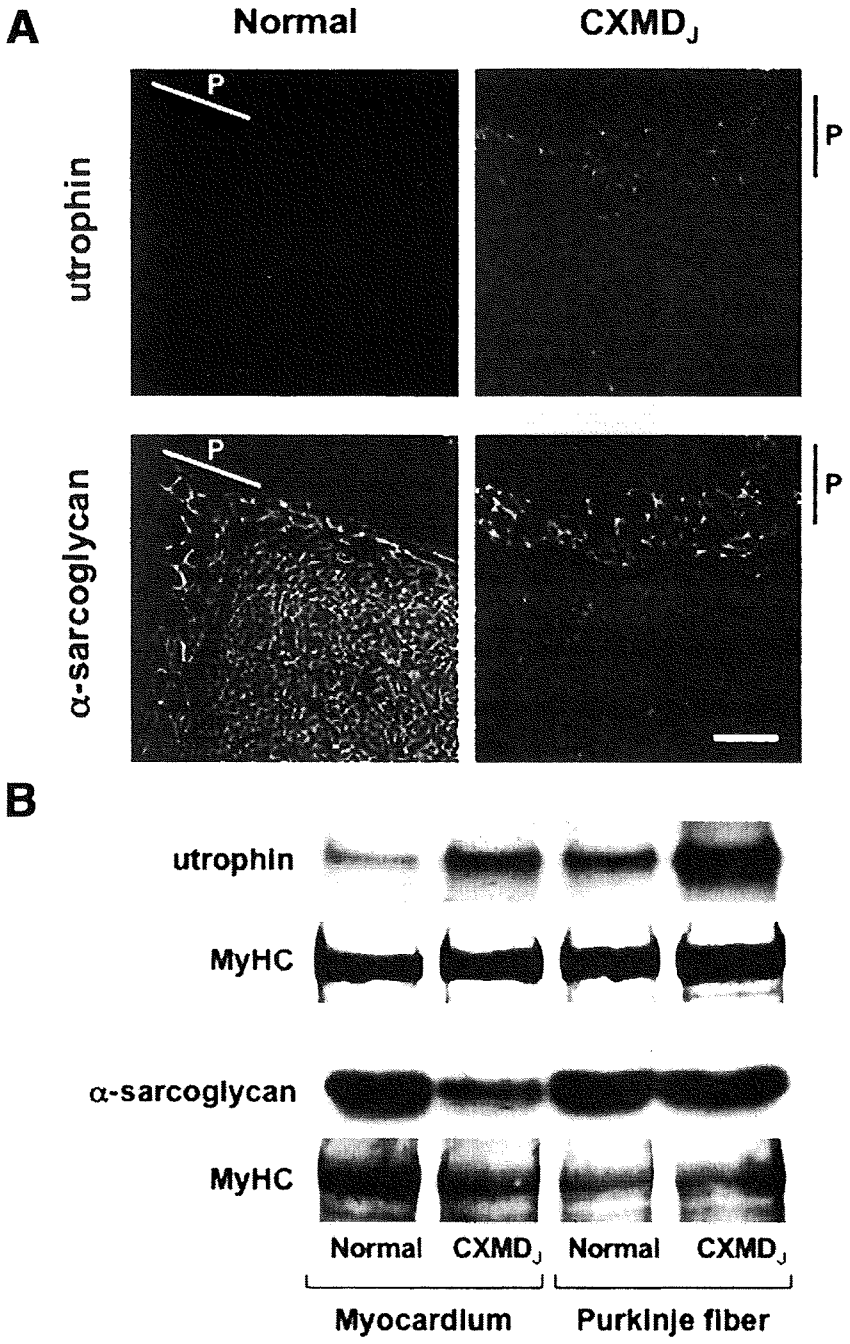

Figure 4. Expression of utrophin and DAPs in ventricular myocardium and Purkinje fibers. A, Immunohistochemical analysis of utrophin and α-sarcoglycan in the LV from normal (III-E01MN in the Table) and affected (III-E02MA in the Table) 4-month-old dogs. Serial cross sections from the LV were stained with antibodies against utrophin (UT-2) or α-sarcoglycan (α-SG2). P indicates Purkinje fibers. Bar = 100 μm. B, Immunoblot analyses using the anti-utrophin (UT-2) or α-sarcoglycan (α-SG2) antibodies. Myosin heavy chain (MyHC) was used as the loading control. Samples from the dogs shown in A were separated by SDS-PAGE on a 7.5% acrylamide gel for utrophin or 9% for α-sarcoglycan.

Degradation of μ-Calpain–Sensitive Myofibrillar Proteins in Purkinje Fibers and Serum of CXMD$_J$

To determine why μ-calpain upregulation leads to degeneration of CXMD$_J$ Purkinje fibers, we investigated the μ-calpain substrate. Desmin, cardiac troponin T, and cardiac troponin I have been identified as μ-calpain–sensitive myofibrillar proteins.[36] Therefore, we investigated whether these molecules are degraded in CXMD$_J$ Purkinje fibers. Immunoblot analyses using microdissected samples indicated that desmin, cardiac troponin T, and cardiac troponin I were degraded in the Purkinje fibers of a CXMD$_J$ at 4 months of age (Figure 7A). Moreover, we found that serum cardiac troponin I was degraded in the previously reported 9-month-old CXMD$_J$ who died suddenly[14] but not in an aged-matched normal dog (Figure 7B).

Discussion

Degeneration of Dystrophin-Deficient Purkinje Fibers Precedes Myocardial Lesion

We report that the characteristic vacuolar degeneration of dystrophin-deficient Purkinje fibers was consistently observed in CXMD$_J$ by 4 months of age. In normal Purkinje fibers, regular round vacuoles are often seen because the myofibrils in cardiac Purkinje fibers are relatively sparse and mainly arranged in thick layers variously near the cell membrane. Larger fibril-free sarcoplasmic regions, therefore,

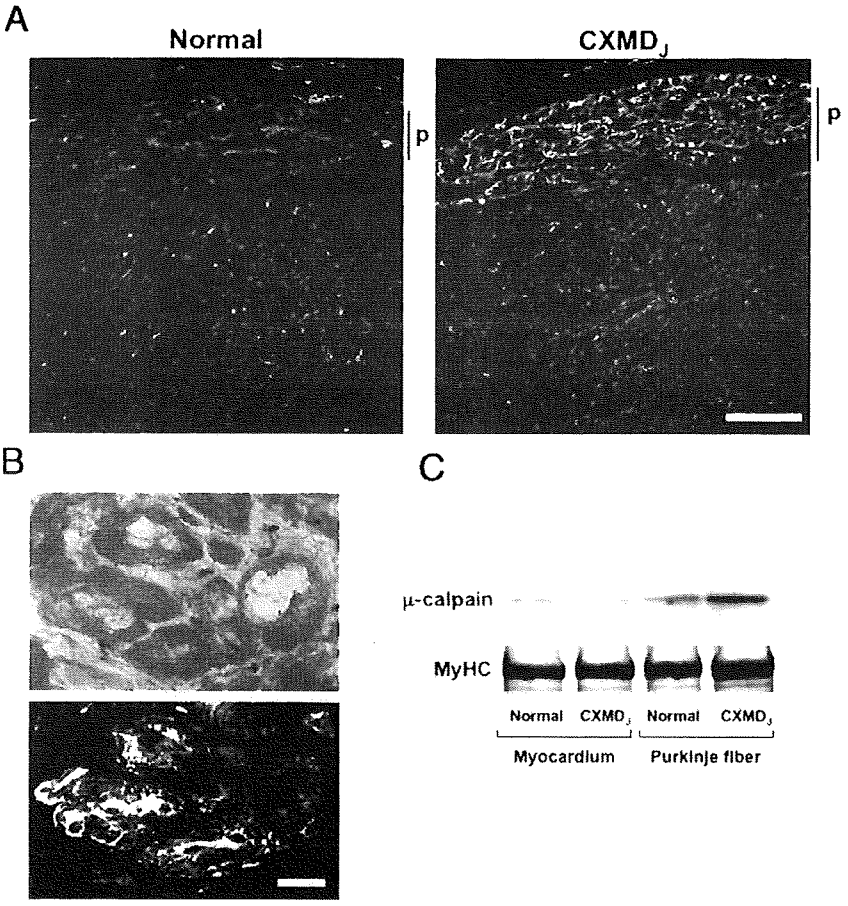

Figure 5. Expression of μ-calpain in LV of normal and CXMD$_J$ dogs. A, Immunohistochemical staining using the anti-μ-calpain antibody (anti-calpain 1 large subunit domain IV) of the LV of normal (III-E01MN in the Table) and affected (III-E02MA in the Table) 4-month-old dogs. P indicates Purkinje fibers. Bar=100 μm. B, Hematoxylin and eosin staining (top panel) and immunohistochemical staining of μ-calpain (bottom panel) of vacuolated Purkinje fibers from the affected dog shown in A. Bar=25 μm. C, Immunoblot analysis of μ-calpain expression. Samples from the dogs shown in A were separated by SDS-PAGE on a 7.5% acrylamide gel. The antibody specific to μ-calpain recognized strong expression of the 82-kDa band in affected Purkinje fibers. Myosin heavy chain (MyHC) was used as the loading control.

look like vacuole structure in normal human and canine heart at the microscopic level.[37] On the other hand, the vacuoles we found in CXMD$_J$ were irregular, and the changes were extensive and progressive. In addition, electron microscopy revealed that dystrophin-deficient Purkinje fibers had severely disrupted myofibrils, suggesting that the vacuoles were the ruins of myofibrillar structures.

We have recently reported that the onset of degeneration of the myocardium in CXMD$_J$ is not detected before 5 months of age.[14] Given these results, it is obvious that the vacuolar degeneration of CXMD$_J$ Purkinje fiber precedes the myocardial lesion. The pathological features of DMD cardiomyopathy have been well characterized,[6] but reports of morphological changes in the conduction systems are very limited. To our knowledge, only 2 reports have described the degeneration of Purkinje fibers.[7,9] However, these studies reported autopsies of DMD patients, and degeneration of the ventricular myocardium was also prominent. Thus, we are able to demonstrate for the first time that selective vacuolar degeneration of Purkinje fibers begins in the early stage of dystrophin deficiency.

Overexpression of Dp71 Might Lead to Degeneration of Dystrophin-Deficient Purkinje Fibers Through Dislocation of Utrophin

Our study also showed that overexpression of Dp71 at the sarcolemma occurred concurrently with vacuolar degeneration of dystrophin-deficient Purkinje fibers. Indeed, previous transgenic mouse studies indicated that overexpression of Dp71[34,38] as well as Dp116[39] damaged or exacerbated normal or *mdx* mice skeletal muscle pathology. Dp71 and Dp116 are C-terminal isoforms of dystrophin and contain cysteine-rich and C-terminal domains that bind to DAP complexes, but both isoforms lack the rod and actin-binding domains of dystrophin. Therefore, Dp71 cannot link to the sarcolemma and actin cytoskeleton. Previous transgenic mouse studies demonstrated that muscle damage is caused by competition between Dp71 or Dp116 and dystrophin or utrophin at the sarcolemma.[34,38,39] In our study, utrophin expression was upregulated in 1- and 2-month-old CXMD$_J$ Purkinje fibers, but the upregulation decreased rapidly in 4-month-old CXMD$_J$. The overexpression of Dp71 might be involved in the mechanism for the dislocation of utrophin, giving rise to Purkinje fiber degeneration.

μ-Calpain Accumulation and Translocation Are Involved in Degeneration of Dystrophin-Deficient Purkinje Fibers

Our study showed that expression of μ-calpain, one of the Ca^{2+}-dependent cysteine proteases, accumulated significantly near the sarcolemma or in the rims of vacuoles and that μ-calpain–sensitive proteins were degraded in CXMD$_J$ Purkinje fibers. Previous studies indicated an increase in Ca^{2+} permeability and subsequent μ-calpain activation and translocation at the sarcolemma in dystrophin-deficient muscle fibers[24,40] and suggested that the activation of μ-calpain may

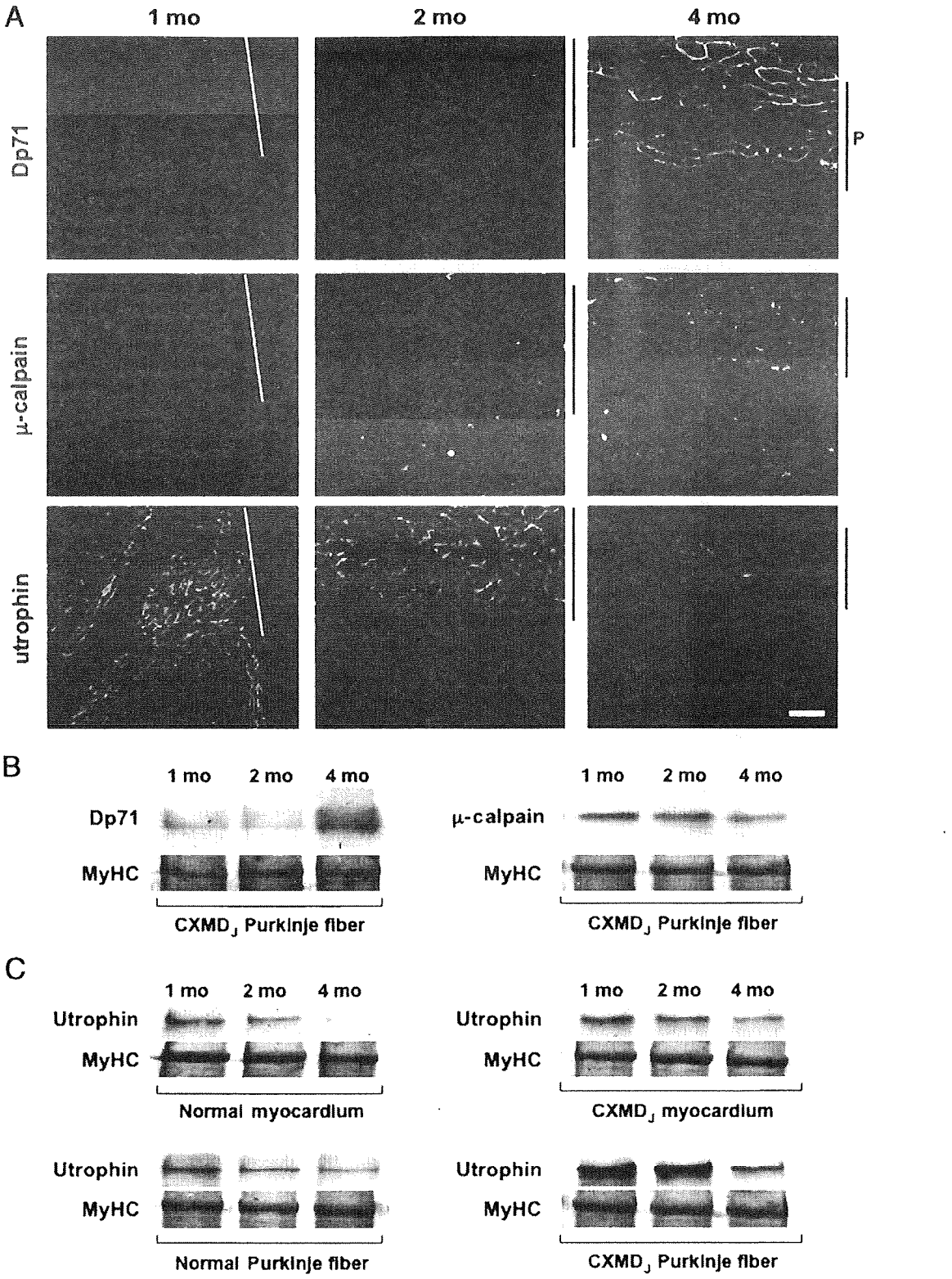

Figure 6. Expression of Dp71, μ-calpain, and utrophin in the LV of CXMD$_J$ pups. A, Serial cryosections from the LV of 1-, 2-, and 4-month-old affected dogs (III-203MA, III-202MA, and III-E02MA in the Table, respectively) were stained with antibodies against dystrophin C-terminal (NCL-DYS2), μ-calpain (anti-calpain 1 large subunit domain IV), or utrophin (UT-2). P indicates Purkinje fibers. Bar=50 μm. B, Immunoblot analyses of Purkinje fibers for Dp71 and μ-calpain. Samples of Purkinje fibers of the affected dogs shown in A were separated by SDS-PAGE on a 9% acrylamide gel and stained with antibodies against dystrophin C-terminal (NCL-DYS2) or μ-calpain (anti-calpain 1 large subunit domain IV). Myosin heavy chain (MyHC) was used as the loading control. C, Immunoblot analysis using anti-utrophin antibody (UT-2). Samples from the ventricular myocardium and Purkinje fibers of the normal (III-204MN, III-E09MN, and III-E01MN in the Table, respectively) and affected 1-, 2-, and 4-month-old dogs shown in A were separated by SDS-PAGE on a 9% acrylamide gel. MyHC was used as the loading control.

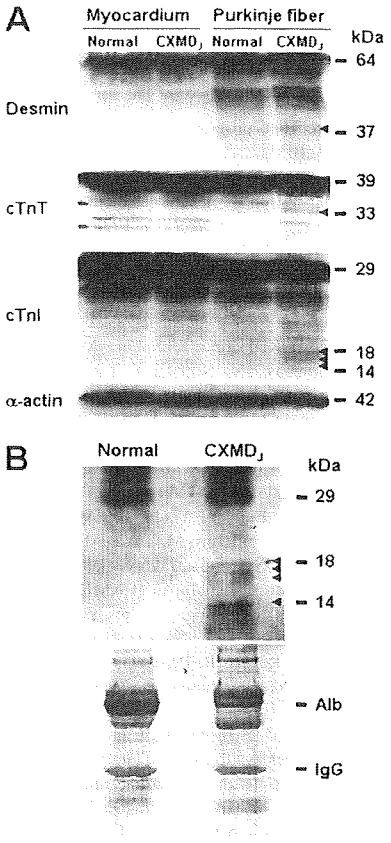

Figure 7. Degradation of μ-calpain–sensitive proteins in Purkinje fibers of CXMD$_J$. A, Immunoblot analyses of μ-calpain–sensitive proteins (desmin, cardiac troponin T [cTnT], and cardiac troponin I [cTnI]) and internal control (α-sarcomeric actin) in the microdissected myocardium and Purkinje fiber of the normal dog (III-2006FN in the Table) and CXMD$_J$ (III-1903MA in the Table). Arrowheads indicate degradation forms of each molecule. B, Immunoblot analysis of cardiac troponin I in the serum of a 9-month-old CXMD$_J$ who died a sudden death (III-D55MA in the Table) (top panel). Arrowheads show degraded forms of cardiac troponin I. Albumin (Alb) and immunoglobulin G (IgG) are shown in a Coomassie Brilliant Blue staining of the same blotting membrane (bottom panel).

contribute to the pathogenesis in fibrillating human atria.[23] Moreover, it has been reported that proteolysis near the sarcolemmal ruptures increases the activity of calcium leak channels.[41] It is therefore intriguing that accumulation of μ-calpain was closely related to the appearance of vacuolar degeneration of CXMD$_J$ Purkinje fibers. Translocation to the membrane might be one of the important steps in the regulation of enzymatic activities of calpains. A previous report showed that calpain is present in the cytosol in an uncleaved, inactive state, but it is translocated to the membrane on a rise in the intracellular Ca^{2+} concentration and is activated at the cell membrane.[42] Hence, our results of calpain accumulation and translocation to the subsarcolemma are important to understanding the degeneration of dystrophin-deficient Purkinje fibers.

Purkinje fibers are uniquely differentiated muscle cells that have the same origin as ventricular myocardial cells.[43] It is not, however, clear why dystrophin deficiency preferentially affects Purkinje fibers. It is well known that fewer myofibrils and the absence of a T-tubule system are characteristic of Purkinje fibers.[16,37] Previous study of stimulation-evoked Ca^{2+} transients showed that the earliest rise in Ca^{2+} occurred at the subsarcolemma in atrial myocytes, which have a poorly developed T-tubule system.[44]

In turn, Iwata et al[45] recently reported translocation of the Ca^{2+}-permeable growth factor–regulated channel from the cytoplasm to the sarcolemma in *mdx* cardiac and skeletal muscle. Moreover, stretch-activated channels were reported to be involved in calcium-handling abnormalities in older *mdx* mice that presented with abnormal calcium transients and increased protein expression of the ryanodine receptor,[46] implying the participation of the stretch-activated channels even in younger *mdx* mice. In addition, IP3-dependent calcium release has been shown to be involved in calcium imbalance in dystrophin-deficient cultured myotube.[47] Other than the physiological Ca^{2+} transient in Purkinje fibers, which lack a T-tubule system, abnormal Ca^{2+} channels possibly affect subsarcolemmal Ca^{2+} homeostasis in dystrophin-deficient Purkinje fibers.

Degeneration of Purkinje Fibers Might Be Associated With ECG Abnormalities or Crucial Ventricular Arrhythmias in Dystrophinopathies

We recently showed that characteristic deep Q waves were found in CXMD$_J$, and this finding preceded posterobasal myocardial fibrosis.[14] In normal LV, the initial QRS vector is oriented to the right, anteriorly, usually superiorly, and gives rise to small negative q waves. Septal q waves were prominent in dystrophin-deficient heart. Indeed, the deep septal q (distinct deep Q) waves are mainly developed not only in leads II, III, and aVF in CXMD$_J$[14] and GRMD[11] but also in leads I, aVL, and V_5 to V_6 in human DMD.[6] The degeneration of Purkinje fibers might cause a delay of depolarization at the posterobasal region, resulting in distinct deep Q waves, although we need to carefully rule out degeneration of the myocardium itself at further molecular levels. It is noteworthy that 10 of 12 patients with muscular dystrophy, including 6 with DMD and Becker muscular dystrophy, had a prolonged His-ventricular interval, which indicates a delay of the His-Purkinje system.[48]

We and other researchers have suggested that the lack of specific membrane proteins might modulate particular ionic current, resulting in ECG changes. It has been reported recently that the expression of the cardiac sodium channel Nav1.5 has been altered and sodium current decreased in the heart of *mdx* 5cv mice, which may explain the alterations in cardiac conduction in dystrophin deficiency.[49]

In our dystrophic dog colony, one 9-month-old CXMD$_J$ developed ventricular arrhythmia and experienced a sudden death, the details of which were described in our recent report.[14] To evaluate the arrhythmias in CXMD$_J$ colony, we performed Holter monitoring and found that 1 CXMD$_J$ dog frequently showed nonsustained ventricular tachycardia (N.U. and N. Yugeta, DVM, PhD, unpublished data, 2003). In DMD, sudden death, presumed to be associated with ventricular arrhythmias, was not rare.[8] Cardiac conduction blocks, such as atrioventricular block, bundle-branch block, and fascicular block, were a common complication in the

disease.[7-9] It is intriguing to note that a part of the His bundle and bundle branches as well as terminal Purkinje fibers is composed of cardiac Purkinje cells. Therefore, the conduction delay in the His-Purkinje system or conduction block due to the degeneration of Purkinje fibers may underlie the generation of ventricular arrhythmias in dystrophin deficiency. In addition, a case report describes sustained bundle branch reentry ventricular tachycardia in Becker muscular dystrophy, for which the patient underwent radiofrequency catheter ablation of the right bundle branch.[50] Evaluation of Purkinje fibers in DMD heart may shed light on the relationship between the degeneration of Purkinje fibers and development of arrhythmias.

Acknowledgments

We would like to thank M. Yoshimura, Y. Itoh, and R. Nakagawa (Department of Molecular Therapy) for their technical assistance; K. Sugie, F. Uematsu, I. Nishino (Department of Neuromuscular Research), and Y. Kozuka (Department of Ultrastructural Research, National Institute of Neuroscience) for their help in electron microscopy; Y. Fujii and N. Yugeta (Department of Surgery I, Azabu University) for their support in ECG and echocardiographic evaluations; and M. Imamura, M. Yoshida (Department of Molecular Therapy, National Institute of Neuroscience), G.E. Morris (Wolfson Centre for Inherited Neuromuscular Disease), and H. Sorimachi (Tokyo Metropolitan Institute of Medical Science) for providing antibodies.

Sources of Funding

This work is supported by Grants-in-Aid from the Center of Excellence, Research on Nervous and Mental Disorders (10B-1, 13B-1, 16B-2, 19A-7), Health Science Research Grants for Research on Psychiatry and Neurological Disease and Mental Health (H12-kokoro-025, H15-kokoro-021, H18-kokoro-019), Human Genome and Gene Therapy (H10-genome-015, H13-genome-001, H16-genome-003), Health and Labor Sciences Research Grants for Translation Research (H19-translational research-003) from the Ministry of Health, Labor, and Welfare of Japan, and a Grant-in-Aid for Scientific Research from the Ministry of Education, Science, Sports, and Culture of Japan to Dr Shimatsu (16500283). Dr Nakamura (16590819, 19500375), and Dr Takeda (15390281).

Disclosures

None.

References

1. Koenig M, Hoffman EP, Bertelson CJ, Monaco AP, Feener C, Kunkel LM. Complete cloning of the Duchenne muscular dystrophy (DMD) cDNA and preliminary genomic organization of the DMD gene in normal and affected individuals. *Cell*. 1987;50:509–517.
2. Sadoulet-Puccio HM, Kunkel LM. Dystrophin and its isoforms. *Brain Pathol*. 1996;6:25–35.
3. Campbell KP. Three muscular dystrophies: loss of cytoskeleton-extracellular matrix linkage. *Cell*. 1995;80:675–679.
4. Hirst RC, McCullagh KJ, Davies KE. Utrophin upregulation in Duchenne muscular dystrophy. *Acta Myol*. 2005;24:209–216.
5. Lanfossi M, Cozzi F, Bugini D, Colombo S, Scarpa P, Morandi L, Galbiati S, Cornelio F, Pozza O, Mora M. Development of muscle pathology in canine X-linked muscular dystrophy, I: delayed postnatal maturation of affected and normal muscle as revealed by myosin isoform analysis and utrophin expression. *Acta Neuropathol*. 1999;97:127–138.
6. Perloff JK, Roberts WC, de Leon AC Jr, O'Doherty D. The distinctive electrocardiogram of Duchenne's progressive muscular dystrophy: an electrocardiographic-pathologic correlative study. *Am J Med*. 1967;42:179–188.
7. Sanyal SK, Johnson WW. Cardiac conduction abnormalities in children with Duchenne's progressive muscular dystrophy: electrocardiographic features and morphologic correlates. *Circulation*. 1982;66:853–863.
8. Yanagisawa A, Miyagawa M, Yotsukura M, Tsuya T, Shirato C, Ishihara T, Aoyagi T, Ishikawa K. The prevalence and prognostic significance of arrhythmias in Duchenne type muscular dystrophy. *Am Heart J*. 1992;124:1244–1250.
9. Nomura H, Hizawa K. Histopathological study of the conduction system of the heart in Duchenne progressive muscular dystrophy. *Acta Pathol Jpn*. 1982;32:1027–1033.
10. Valentine BA, Cooper BJ, de Lahunta A, O'Quinn R, Blue JT. Canine X-linked muscular dystrophy: an animal model of Duchenne muscular dystrophy: clinical studies. *J Neurol Sci*. 1988;88:69–81.
11. Moise NS, Valentine BA, Brown CA, Erb HN, Beck KA, Cooper BJ, Gilmour RF. Duchenne's cardiomyopathy in a canine model: electrocardiographic and echocardiographic studies. *J Am Coll Cardiol*. 1991;17:812–820.
12. Shimatsu Y, Katagiri K, Furuta T, Nakura M, Tanioka Y, Yuasa K, Tomohiro M, Kornegay JN, Nonaka I, Takeda S. Canine X-linked muscular dystrophy in Japan (CXMDJ). *Exp Anim*. 2003;52:93–97.
13. Shimatsu Y, Yoshimura M, Yuasa K, Urasawa N, Tomohiro M, Nakura M, Tanigawa M, Nakamura A, Takeda S. Major clinical and histopathological characteristics of canine X-linked muscular dystrophy in Japan, CXMDJ. *Acta Myol*. 2005;24:145–154.
14. Yugeta N, Urasawa N, Fujii Y, Yoshimura M, Yuasa K, Wada MR, Nakura M, Shimatsu Y, Tomohiro M, Takahashi A, Machida N, Wakao Y, Nakamura A, Takeda S. Cardiac involvement in Beagle-based canine X-linked muscular dystrophy in Japan (CXMDJ): electrocardiographic, echocardiographic, and morphologic studies. *BMC Cardiovasc Disord*. 2006;6:47.
15. Bies RD, Friedman D, Roberts R, Perryman MB, Caskey CT. Expression and localization of dystrophin in human cardiac Purkinje fibers. *Circulation*. 1992;86:147–153.
16. Klietsch R, Ervasti JM, Arnold W, Campbell KP, Jorgensen AO. Dystrophin-glycoprotein complex and laminin colocalize to the sarcolemma and transverse tubules of cardiac muscle. *Circ Res*. 1993;72:349–360.
17. Pons F, Robert A, Fabbrizio E, Hugon G, Califano JC, Fehrentz JA, Martinez J, Mornet D. Utrophin localization in normal and dystrophin-deficient heart. *Circulation*. 1994;90:369–374.
18. Rivier F, Robert A, Hugon G, Bonet-Kerrache A, Nigro V, Fehrentz JA, Martinez J, Mornet D. Dystrophin and utrophin complexed with different associated proteins in cardiac Purkinje fibres. *Histochem J*. 1999;31:425–432.
19. Petrof BJ, Shrager JB, Stedman HH, Kelly AM, Sweeney HL. Dystrophin protects the sarcolemma from stresses developed during muscle contraction. *Proc Natl Acad Sci U S A*. 1993;90:3710–3714.
20. Duncan CJ. Role of intracellular calcium in promoting muscle damage: a strategy for controlling the dystrophic condition. *Experientia*. 1978;34:1531–1535.
21. Yeung EW, Whitehead NP, Suchyna TM, Gottlieb PA, Sachs F, Allen DG. Effects of stretch-activated channel blockers on $[Ca^{2+}]_i$ and muscle damage in the mdx mouse. *J Physiol*. 2005;562:367–380.
22. Turner PR, Schultz R, Ganguly B, Steinhardt RA. Proteolysis results in altered leak channel kinetics and elevated free calcium in mdx muscle. *J Membr Biol*. 1993;133:243–251.
23. Goette A, Arndt M, Rocken C, Staack T, Bechtloff R, Reinhold D, Huth C, Ansorge S, Klein HU, Lendeckel U. Calpains and cytokines in fibrillating human atria. *Am J Physiol*. 2002;283:H264–H272.
24. Spencer MJ, Croall DE, Tidball JG. Calpains are activated in necrotic fibers from mdx dystrophic mice. *J Biol Chem*. 1995;270:10909–10914.
25. Lev M, Bharati S. A method of study of the pathology of the conduction system for electrocardiographic and His bundle electrogram correlations. *Anat Rec*. 1981;201:43–49.
26. Le TT, Nguyen TM, Love DR, Helliwell TR, Davies KE, Morris GE. Monoclonal antibodies against the muscle-specific N-terminus of dystrophin: characterization of dystrophin in a muscular dystrophy patient with a frameshift deletion of exons 3–7. *Am J Hum Genet*. 1993;53:131–139.
27. Noguchi S, Wakabayashi E, Imamura M, Yoshida M, Ozawa E. Developmental expression of sarcoglycan gene products in cultured myocytes. *Biochem Biophys Res Commun*. 1999;262:88–93.
28. Imamura M, Ozawa E. Differential expression of dystrophin isoforms and utrophin during dibutyryl-cAMP-induced morphological differentiation of rat brain astrocytes. *Proc Natl Acad Sci U S A*. 1998;95:6139–6144.
29. Araishi K, Sasaoka T, Imamura M, Noguchi S, Hama H, Wakabayashi E, Yoshida M, Hori T, Ozawa E. Loss of the sarcoglycan complex and

sarcospan leads to muscular dystrophy in beta-sarcoglycan-deficient mice. *Hum Mol Genet*. 1999;8:1589–1598.
30. Banks RE, Dunn MJ, Forbes MA, Stanley A, Pappin D, Naven T, Gough M, Harnden P, Selby PJ. The potential use of laser capture microdissection to selectively obtain distinct populations of cells for proteomic analysis: preliminary findings. *Electrophoresis*. 1999;20:689–700.
31. Hagiwara Y, Sasaoka T, Araishi K, Imamura M, Yorifuji H, Nonaka I, Ozawa E, Kikuchi T. Caveolin-3 deficiency causes muscle degeneration in mice. *Hum Mol Genet*. 2000;9:3047–3054.
32. Mizuno Y, Yoshida M, Yamamoto H, Hirai S, Ozawa E. Distribution of dystrophin isoforms and dystrophin-associated proteins 43DAG (A3a) and 50DAG (A2) in various monkey tissues. *J Biochem*. 1993;114:936–941.
33. Sharp N, Kornegay J, Van Camp S, Herbstreith M, Secore S, Kettle S, Hung W, Constantinou C, Dykstra M, Roses A, Bartlett R. An error in dystrophin mRNA processing in golden retriever muscular dystrophy, an animal homologue of Duchenne muscular dystrophy. *Genomics*. 1992;13:115–121.
34. Cox GA, Sunada Y, Campbell KP, Chamberlain JS. Dp71 can restore the dystrophin-associated glycoprotein complex in muscle but fails to prevent dystrophy. *Nat Genet*. 1994;8:333–339.
35. Kameya S, Araki E, Katsuki M, Mizota A, Adachi E, Nakahara K, Nonaka I, Sakuragi S, Takeda S, Nabeshima Y. Dp260 disrupted mice revealed prolonged implicit time of the b-wave in ERG and loss of accumulation of beta-dystroglycan in the outer plexiform layer of the retina. *Hum Mol Genet*. 1997;6:2195–2203.
36. Barta J, Tóth A, Édes U, Vaszily M, Papp JG, Varró A, Papp Z. Calpain-1-sensitive myofibrillar proteins of the human myocardium. *Mol Cell Biochem*. 2005;278:1–8.
37. Tawara S. *The Conduction System of the Mammalian Heart: An Anatomico-Histological Study of the Atrioventricular Bundle and the Purkinje Fibers*. London, UK: Imperial College Press; 2000.
38. Greenberg DS, Sunada Y, Campbell KP, Yaffe D, Nudel U. Exogenous Dp71 restores the levels of dystrophin associated proteins but does not alleviate muscle damage in mdx mice. *Nat Genet*. 1994;8:340–344.
39. Judge LM, Haraguchiln M, Chamberlain JS. Dissecting the signaling and mechanical functions of the dystrophin-glycoprotein complex. *J Cell Sci*. 2006;119:1537–1546.
40. Spencer MJ, Tidball JG. Calpain translocation during muscle fiber necrosis and regeneration in dystrophin-deficient mice. *Exp Cell Res*. 1996;226:264–272.
41. McCarter GC, Steinhardt RA. Increased activity of calcium leak channels caused by proteolysis near sarcolemmal ruptures. *J Membr Biol*. 2000;176:169–174.
42. Saido TC, Suzuki H, Yamazaki H, Tanoue K, Suzuki K. In situ capture of m-calpain activation in platelets. *J Biol Chem*. 1993;268:7422–7426.
43. Kanzawa N, Poma CP, Takebayashi-Suzuki K, Díaz KG, Layliev J, Mikawa T. Competency of embryonic cardiomyocytes to undergo Purkinje fiber differentiation is regulated by endothelin receptor expression. *Development*. 2002;129:3185–3194.
44. Tanaka H, Masumiya H, Sekine T, Kase J, Kawanishi T, Hayakawa T, Miyata S, Sato Y, Nakamura R, Shigenobu K. Involvement of Ca^{2+} waves in excitation-contraction coupling of rat atrial cardiomyocytes. *Life Sci*. 2001;70:715–726.
45. Iwata Y, Katanosaka Y, Arai Y, Komamura K, Miyatake K, Shigekawa M. A novel mechanism of myocyte degeneration involving the Ca^{2+}-permeable growth factor-regulated channel. *J Cell Biol*. 2003;161:957–967.
46. Williams IA, Allen DG. Intracellular calcium handling in ventricular myocytes from mdx mice. *Am J Physiol*. 2007;292:H846–H855.
47. Balghi H, Sebille S, Mondin L, Cantereau A, Constantin B, Raymond G, Cognard C. Mini-dystrophin expression down-regulates IP3-mediated calcium release events in resting dystrophin-deficient muscle cells. *J Gen Physiol*. 2006;128:219–230.
48. Himmrich E, Popov S, Liebrich A, Rosocha S, Zellerhoff C, Nowak B, Przibille O. Hidden intracardiac conduction disturbances and their spontaneous course in patients with progressive muscular dystrophy. *Z Kardiol*. 2000;89:592–598.
49. Gavillet B, Rougier JS, Domenighetti AA, Behar R, Boixel C, Ruchat P, Lehr HA, Pedrazzini T, Abriel H. Cardiac sodium channel Nav1.5 is regulated by a multiprotein complex composed of syntrophins and dystrophin. *Circ Res*. 2006;99:407–414.
50. Negri SM, Cowan MD. Becker muscular dystrophy with bundle branch reentry ventricular tachycardia. *J Cardiovasc Electrophysiol*. 1998;9:652–654.

CLINICAL PERSPECTIVE

In Duchenne muscular dystrophy, a devastating skeletal and cardiac muscle disorder caused by mutations in the dystrophin gene, cardiac failure such as dilated cardiomyopathy and arrhythmia needs to be overcome, although the respiratory management has significantly improved the life span of the patients. Among cardiac involvements, ECG findings such as distinctive deep Q waves have been noted and are ascribed to fibrosis in the posterobasal region of the left ventricle. When Urasawa et al (National Institute of Neuroscience, Tokyo, Japan) examined the hearts of dogs with canine X-linked muscular dystrophy in Japan ($CXMD_J$), an appropriate dystrophin-deficient model of Duchenne muscular dystrophy, the Purkinje fibers showed remarkable vacuolar degeneration as early as 4 months of age despite no detectable fibrotic lesions in ventricular myocardium. The degeneration of $CXMD_J$ Purkinje fibers was coincident with overexpression of Dp71, a C-terminal truncated form of dystrophin, at the sarcolemma and translocation of calcium-dependent protease μ-calpain to the cell periphery near the sarcolemma or in the vacuoles. Utrophin, a homologue of dystrophin, was highly upregulated in the earlier stage of $CXMD_J$ Purkinje fibers, but the expression was dislocated when vacuolar degeneration was recognized at 4 months of age, despite preservation of dystrophin-associated proteins at the sarcolemma. The selective degeneration of Purkinje fibers can be associated with distinct deep Q waves on ECG and the fatal arrhythmia seen in dystrophin deficiency. Further clarification of the molecular mechanism of selective degeneration of Purkinje fibers may shed light on the development of new therapy for cardiac involvement in dystrophin-deficient muscular dystrophy.

THE JOURNAL OF GENE MEDICINE
J Gene Med 2008; **10**: 702–713.
Published online in Wiley InterScience (www.interscience.wiley.com) **DOI**: 10.1002/jgm.1190

RESEARCH ARTICLE

Downstream utrophin enhancer is required for expression of utrophin in skeletal muscle

Jun Tanihata[1,2]
Naoki Suzuki[1,3]
Yuko Miyagoe-Suzuki[1]
Kazuhiko Imaizumi[2]
Shin'ichi Takeda[1]*

[1]*Department of Molecular Therapy, National Institute of Neuroscience, National Center of Neurology and Psychiatry, Ogawa-higashi, Kodaira, Tokyo, Japan*

[2]*Laboratory of Physiological Sciences, Faculty of Human Sciences, Waseda University, Mikajima, Tokorozawa, Japan*

[3]*Department of Neurology, Tohoku University School of Medicine, Seiryo-machi, Sendai, Japan*

*Correspondence to:
Shin'ichi Takeda, Department of Molecular Therapy, National Institute of Neuroscience, National Center of Neurology and Psychiatry, 4-1-1 Ogawa-higashi, Kodaira, Tokyo 187-8502, Japan.
E-mail: takeda@ncnp.go.jp

Received: 17 October 2007
Accepted: 30 January 2008

Abstract

Background Duchenne muscular dystrophy is caused by the absence of the muscle cytoskeletal protein dystrophin. Utrophin is an autosomal homologue of dystrophin, and overexpression of utrophin is expected to compensate for the dystrophin deficit. We previously reported that the 5.4-kb 5′-flanking region of the utrophin gene containing the A-utrophin core promoter did not drive transgene expression in heart and skeletal muscle. To clarify the regulatory mechanism of utrophin expression, we generated a nuclear localization signal-tagged LacZ transgenic (Tg) mouse, in which the LacZ gene was driven by the 129-bp downstream utrophin enhancer (DUE) and the 5.4-kb 5′-flanking region of the utrophin promoter.

Methods Two Tg lines were established. The levels of transgene mRNA expression in several tissues were examined by reverse transcriptase-polymerase chain reaction (RT-PCR) and quantitative RT-PCR. Cryosections of several tissues were stained with haematoxylin and eosin and X-gal.

Results The transgene expression patterns were consistent with endogenous utrophin in several tissues including heart and skeletal muscle. Transgene expression was also up-regulated more in regenerating muscle than in nonregenerating muscle. Moreover, utrophin expression was augmented in the skeletal muscle of DUE Tg/dystrophin-deficient *mdx* mice through cross-breeding experiments. We finally established cultures of primary myogenic cells from this Tg mouse and found that utrophin up-regulation during muscle differentiation depends on the DUE motif.

Conclusions Our results showed that DUE is indispensable for utrophin expression in skeletal muscle and heart, and primary myogenic cells from this Tg mice provide a high through-put screening system for drugs that up-regulate utrophin expression. Copyright © 2008 John Wiley & Sons, Ltd.

Keywords downstream utrophin enhancer; Duchenne muscular dystrophy; dystrophin; transcriptional regulation; transgenic mice; utrophin

Introduction

Duchenne muscular dystrophy (DMD) is an X-linked progressive disorder caused by a defect in the DMD gene, which encodes dystrophin [1]. Dystrophin is a 427-kDa cytoskeletal protein that is normally located on the subsarcolemma and fixed by interaction with dystrophin-associated proteins (DAPs), some of which span the membrane [2–5]. This protein complex links the cytoskeleton of myofibers to the extracellular matrix to

maintain the integrity of the sarcolemma. The lack of dystrophin in DMD causes a secondary loss of DAPs in the sarcolemma and leads to massive muscle necrosis, resulting in cardiomyopathy and early death. Unfortunately, there is no treatment available to stop the progression of this devastating neuromuscular disorder other than corticosteroids. Of the various therapeutic strategies for DMD being developed, up-regulation of utrophin has received considerable attention over recent years.

Utrophin is a 395-kDa cytoskeletal protein with a high degree identity with dystrophin at the amino acid level [6,7] and is an autosomal homologue of dystrophin. It is ubiquitously expressed in most tissues. In embryonic and neonatal skeletal muscles, it is expressed both synaptically and extra-synaptically. In adult skeletal muscle, it is found mostly at the postsynaptic membrane of the neuromuscular junction (NMJ) and the myotendinous junction [8,9].

Mdx mice completely lack the expression of dystrophin, but the signs and symptoms of DMD are not progressive until later in the course of the disease. This mild phenotype can be at least partly explained by up-regulation of utrophin at the sarcolemma [10,11]. Additional studies have shown that utrophin is present in greater amounts in small caliber muscle fibers of *mdx* mice [12,13] and small or regenerating muscle fibers of DMD patients [14,15]. By contrast, utrophin null-*mdx* (dko) mice have a severe myopathic phenotype that is lethal within 20 weeks of birth.

Previous transgenic (Tg) experiments showed that over-expression of utrophin at the sarcolemma compensates for the lack of dystrophin and ameliorates dystrophic phenotypes in dystrophin-deficient *mdx* mice, where components of DAPs had been restored [16–18]. Similarly, adenovirally transduced utrophin ameliorates dystrophic changes in *mdx* mice [19]. We previously reported that the immune response to adenovirally transferred β-galactosidase (β-gal) expression evoked up-regulation of endogenous utrophin, resulting in partial improvement of *mdx* phenotypes [20]. These data suggest that systemic up-regulation of utrophin in DMD patients may lead to an effective treatment for this devastating disorder. However, the regulatory mechanism of utrophin expression is not yet fully understood.

Transcriptional regulation of the utrophin gene is more complicated than previously pictured. Two full-length utrophin mRNAs, A and B, which encode different N-termini, are driven by two distinct promoters [21,22]. Both A- and B-utrophin mRNAs are expressed in a tissue-specific manner, and an immunohistochemical study showed that A-utrophin is expressed in the NMJ, choroid plexus, pia mater, and renal glomerulus and tubule [11]. On the other hand, B-utrophin is expressed in vascular endothelial cells [11]. Several short C-terminal utrophin isoforms have been also reported, as found in dystrophin [23]. To elucidate the transcriptional regulation of the utrophin gene, a more powerful tool is engineering an *in vivo* mouse model carrying a reporter gene. We previously generated a transgenic mouse (Gnls) in which the LacZ gene was driven by the 5385-bp 5′-flanking region containing the A-utrophin promoter [24]. Expression of β-gal protein and mRNA derived from the transgene coincided well with the endogenous expression of utrophin in liver, testis, colon, submandibular gland, and small intestine, but β-gal expression was extremely low in skeletal and cardiac muscle. These results suggested that muscle repressor elements may be present in the 5385-bp region or that another regulatory element outside the region might be required for the expression in striated muscle. Comparable results were found by Weir *et al.* [25] by using a transgene covering 3.8 kb of the mouse promoter region, which included the 1.3-kb reporter sequence characterized by Dennis *et al.* [21].

Recently, the downstream utrophin enhancer (DUE) region was identified and located approximately 9 kb downstream of the second intron. The upstream utrophin promoter is under the control of DUE [10,26]. Therefore, in the present study, we generated transgenic mice (DUE Tg) in which DUE was added upstream of the 5385-bp 5′-flanking region and analysed the expression pattern of the transgene in several tissues. We found that the LacZ genes were expressed in skeletal and cardiac muscles. These data are very relevant to finding a way to up-regulate utrophin expression, and DUE mice as well as the primary cells derived from the mice are available for that purpose.

Materials and methods

Construction of transgene and generation of transgenic mice

To further investigate the utrophin A promoter activity in our previous report, genomic fragments containing the 5′ end of the mouse A-utrophin gene were cloned from a 129Sv mouse genomic library (Stratagene, Inc., La Jolla, CA, USA). One clone contained the 5385-bp 5′-flanking region of the A-utrophin gene, the complete exon 1A, and the first 59 bp of the exon 2 untranslated region (UTR). The genomic fragment was fused in-frame to an nls (from SV40T antigen)-tagged LacZ gene [27] (pCMVb; Clontech, San Jose, CA, USA), followed by a rabbit β-globin polyA signal in Bluescript II (Stratagene) [24]. Furthermore, we inserted the 129-bp utrophin enhancer region that is found in utrophin gene intron 2 [26] upstream of this fragment (Figure 1A). The DNA fragment containing the transgene expression cassette was purified from agarose gel and injected into fertilized C57BL/6J eggs by YS Institute (Utsunomiya, Tochigi, Japan) (Figure 1B). We obtained two transgenic F0 (downstream utrophin enhancer/A promoter-nls LacZ transgenic mice), and two transgenic lines were established by mating the founders with C57BL/6J mice (B6) (Figure 1C). To obtain transgenic *mdx* (Tg/*mdx*) male mice, we mated Tg male mice with *mdx* female mice (Figure 1D).

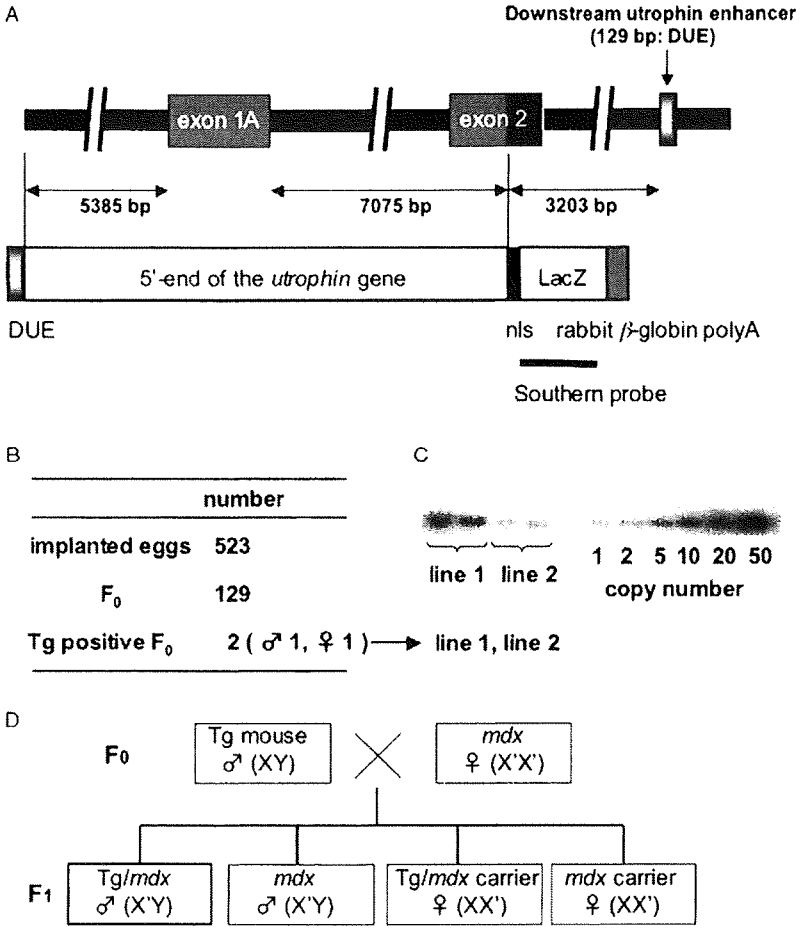

Figure 1. Generation of downstream utrophin enhancer/A-utrophin promoter-nls LacZ Tg mice. (A) Diagram of the transgene used in this study. The genomic fragment (12.9 kb), which contained the 129-bp DUE, 5385-bp 5′-flanking region of the A-utrophin gene, exon 1A, intron 1, and the first 59 bp of exon 2 UTR, was fused in-frame to the nls-tagged LacZ gene. The black bar indicates the Southern probe used to determine genotypes. (B) Summary of generation of Tg mice. (C) Determination of copy numbers in Tg mice by Southern blotting (left). The vector plasmids containing the transgene served as a standard to estimate the number of copies of the transgene (right). (D) Generation of Tg/mdx mice. The bold box indicates the Tg/mdx male mice used in the present study

Animals

C57BL/6J and *mdx* mice aged 5–12 weeks, Tg mice and their wild littermates aged 3–18 weeks, and Tg/*mdx* mice aged 3–7 weeks were used. All animals were housed in a separate room at a temperature of 20–22 °C and under a 12:12 h light/dark cycle. Animals were sacrificed by cervical dislocation. All protocols were approved by the Institutional Animal Care and Use Committee of the National Institute of Neuroscience and were performed in compliance with the 'Guide for the Care and Use of Animals' of the Division of Laboratory Animal Resources.

Genotyping

Tg mice were screened by Southern blotting of genomic DNA from their tails. Genomic DNA was isolated using a lysis buffer [50 mM Tris-HCl, pH 8.0, 0.1 M NaCl, 20 mM ethylenediaminetetraacetic acid, 1% sodium dodecyl sulfate (SDS)] with proteinase K (0.15 mg/ml) and pronase E (1 mg/ml) digestion. Genomic DNA (10 μg) was digested by *BamHI*, separated on a 0.8% agarose gel, and transferred to Hybond-N+ membranes (Amersham Biosciences, Bucks, UK). A 3072-bp DNA fragment of the LacZ gene was labelled with ^{32}P-dCTP as a Southern probe, and hybridized with membranes at 65 °C overnight. The membranes were then washed extensively [2 × saline sodium phosphate-EDTA (SSPE), 0.1% SDS; 1 × SSPE, 0.1% SDS; 0.1 × SSPE, 0.1% SDS] at 65 °C and analysed by BAS 2500 (Fuji Film, Tokyo, Japan).

Isolation of total RNA from mice and myogenic cells

Three- to 8-week-old Tg mice and their wild-type littermates were sacrificed, and tissues were isolated and rapidly frozen in liquid nitrogen. Total RNA was isolated from frozen tissues and myogenic cells using TRIzol reagent (Invitrogen Life Technologies, Carlsbad, CA, USA) according to the manufacturer's protocol.

Reverse transcription-polymerase chain reaction (RT-PCR) and quantitative real-time PCR (q-RT-PCR)

RT was performed with 1.0 μg of total RNA using a QuantiTect Reverse Transcription Kit (Qiagen, Valencia, CA, USA) according to the manufacturer's protocol. PCR was performed using LacZ sense (5′-CGACATTGGCGTAAGTGAAG-3′) and antisense (5′-ATCGCCATTTGACCACTACC-3′) primers for 30 cycles (denaturation at 95 °C for 1 min, annealing at 60 °C for 30 s, and extension at 72 °C for 1 min). As a control for the generation of PCR products due to residual contamination of genomic DNA, an equivalent amount of RNA that had not been treated with RT was also processed in parallel. The RT-PCR products of all samples were compared with the levels of a housekeeping gene, 18 s rRNA, amplified with the following primer pair: sense (5′-TACCCTGGCGGTGGGATTAAC-3′) and anti-sense (5′-CGAGAGAAGACCACGCCAAC-3′) primers. The levels of various cDNAs were determined by q-RT-PCR using SYBR Green from ABI PRISM 7700 (Applied Biosystems, Foster City, CA, USA). Each result shows the average of three or four samples. The LacZ and 18 s rRNA primer sequences are described above. A-utrophin: sense (5′-ATGGCCAAGTATGGGGACCTTG-3′) and anti-sense (5′-GTGGTGAAGTTGAGGACGTTGAC-3′) primers; myogenin: sense (5′-CATGGTGCCCAGTGAATGCAACTC-3′) and anti-sense (5′-TATCCTCCACCGTGATGCTGTCCA-3′) primers; and MEF2C: sense (5′-TGGACAACAAAGCCCTC-AGCAGGT-3′) and anti-sense (5′-AATCCCTGCTTCGTTC-CCTCTGC-3′) primers were designed for q-RT-PCR. 18 s rRNA mRNA was amplified as an internal control.

Histochemical analysis

After Tg and wild-type mice were sacrificed, the cerebrum, cerebellum, submandibular gland, lung, liver, kidney, small intestine, colon, testis, tibialis anterior (TA) and gastrocnemius (GC) muscles, diaphragm, and heart were isolated and frozen in liquid nitrogen-cooled isopentane. Cryosections (7 μm) from several tissues were stained with haematoxylin and eosin (H&E) and with 5-bromo-4-chloro-3-indolyl-β-D-galactopyranoside (X-gal; Wako Chemicals, Osaka, Japan) as described previously [28]

Immunohistochemistry

Serial transverse cryosections (7 μm) from different tissues were placed on slides, then dried and fixed in acetone for 10 min at −20 °C. We carried out immunohistochemical analysis with a rabbit polyclonal antibody against human utrophin (UT-2) that recognizes amino acid positions 1768–2078 [29]. The primary antibodies were detected with Alexa 488-labelled goat anti-rabbit IgG (Molecular Probes, Eugene, OR, USA). The nucleus was stained with TOTO-3 iodide (Molecular Probes). The NMJ was stained with Alexa 594-labelled α-bungarotoxin (α-BTX) (Molecular Probes). Signals were recorded photographically with a laser-scanning confocal imaging system (TCSSP; Leica Microsystems, Wetzlar, Germany).

Cardiotoxin injection

To cause muscle degeneration, we injected 100 μl of cardiotoxin (CTX) of *Naja naja atra* venom (10 μM in saline; Wako Chemicals) into the right TA and GC muscles of 5- to 7-week-old Tg mice using a 29-gauge needle. The concentration of CTX was determined as described previously [30]. CTX-injected Tg mice were sacrificed 1–14 days after injection. The CTX-injected and contralateral non-injected TA and GC muscles were isolated and frozen in liquid nitrogen-cooled isopentane. Cryosections (7 μm) were stained with H&E and X-gal. At the same time, serial cryosections (7 μm) were stained with UT-2 together with Alexa 594-labelled α-BTX. Total RNA was isolated from these frozen tissues.

Cell preparation and culture

Mouse-derived mononucleated cells were prepared from DUE and Gnls Tg mice and C57BL/6J mice as previously described [31]. Primary myoblasts were cultured alone with growth medium (GM): F-10 containing 20% fetal bovine serum, 1% penicillin-streptomycin (Invitrogen), and 2.5 ng/ml basic fibroblast growth factor (Invitrogen) in collagen-coated dishes (Iwaki, Tokyo, Japan) or chamber slides (Nalge Nunc, Rochester, NY, USA) coated with collagen type I (Upstate, Waltham, MA, USA). For differentiation, the medium was changed to a differentiation medium (DM; 5% horse serum in Dulbecco's modified Eagle's medium) and cultured 5 days. GM and DM were replenished every 24 h [32].

Statistical analysis

Statistical differences were determined by Student's unpaired *t*-test. All data are expressed as means ± SE. $p < 0.05$ was considered statistically significant.

Results

Generation of downstream utrophin enhancer/A promoter-nls LacZ transgenic (DUE Tg) mice

Two F0 'founder' mice were identified by Southern blotting analysis using a LacZ cDNA probe, and two transgenic lines were established (Figure 1B). The approximate numbers of transgene copies were

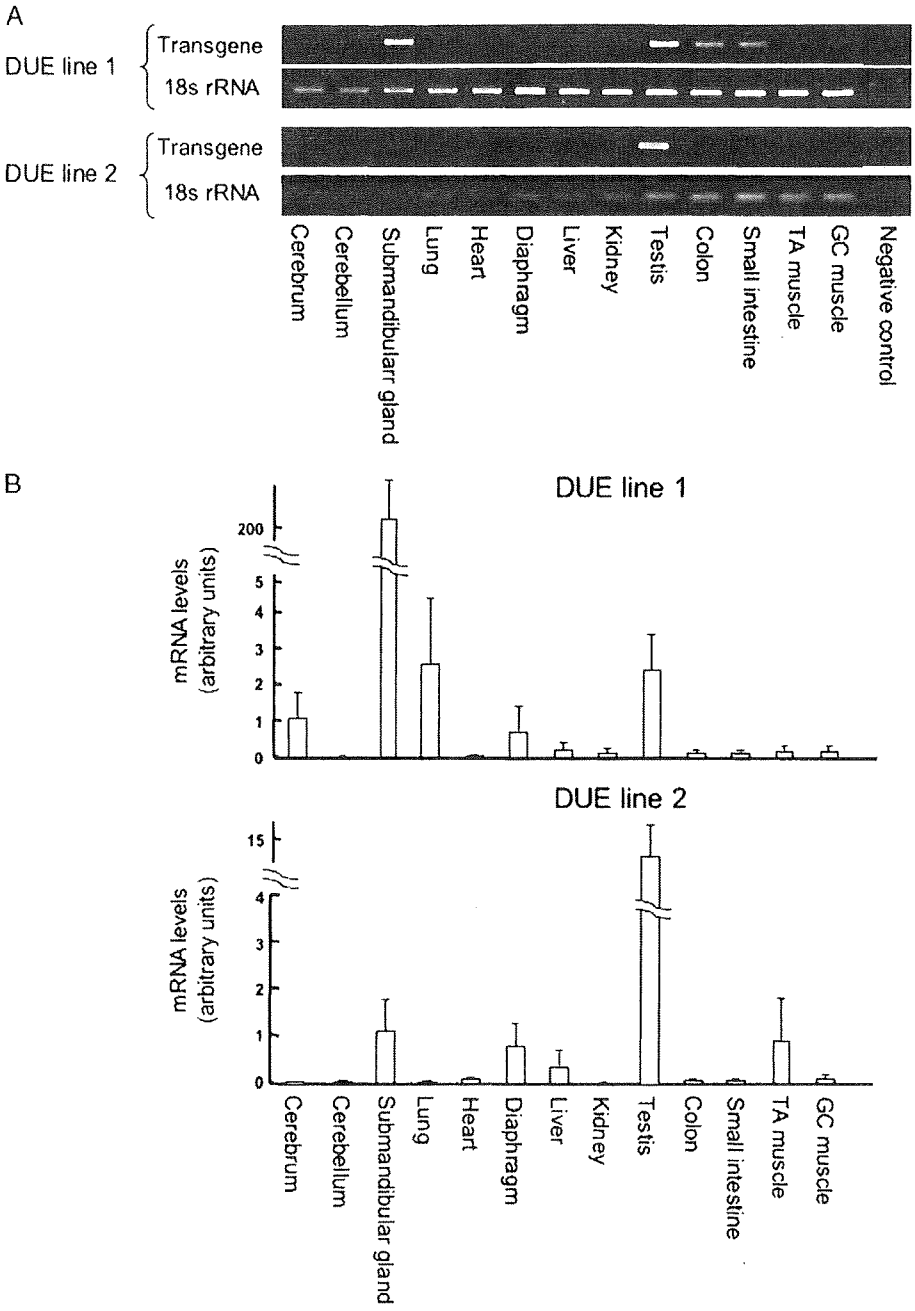

Figure 2. Transgene mRNA expression in several tissues of Tg mice. (A) Representative photomicrographs of EtBr-stained agarose gels depicting cDNA products of the transgene and 18s rRNA from RT-PCR analysis of total RNA from several tissues in Tg mice. (B) Quantification of q-RT-PCR products of the transgene were done by optimization to expression of 18s rRNA in several tissues. The ratio of the transgene to 18s rRNA is shown as the mean ± SEM of four independent experiments performed in triplicate

approximately 15 in line 1 or approximately two in line 2 (Figure 1C).

The levels of transgene expression in several tissues were determined by RT-PCR and q-RT-PCR (Figures 2A and 2B). High levels of transgene mRNA expression were detected in the submandibular gland, testis, lung, colon, and small intestine of DUE line 1 Tg mice and in the submandibular gland and testis of DUE line 2 Tg mice. The signals were weakly detected in other tissues of DUE line 2 Tg mice, probably because there were fewer copies of the transgene.

Comparison of β-gal and endogenous utrophin expression in DUE Tg mice

To compare β-gal expression derived from the transgene with endogenous utrophin expression, cryosections were stained with X-Gal, and then serial cryosections were stained with either H&E or UT-2, a polyclonal antibody against human utrophin [29] (Figure 3). UT-2 recognized only the full-length A- and B-utrophin [29]. We found that β-gal expression coincided well with endogenous utrophin expression in the liver, testis, colon, submandibular gland, small intestine, kidney, and lung (Figure 3A). When

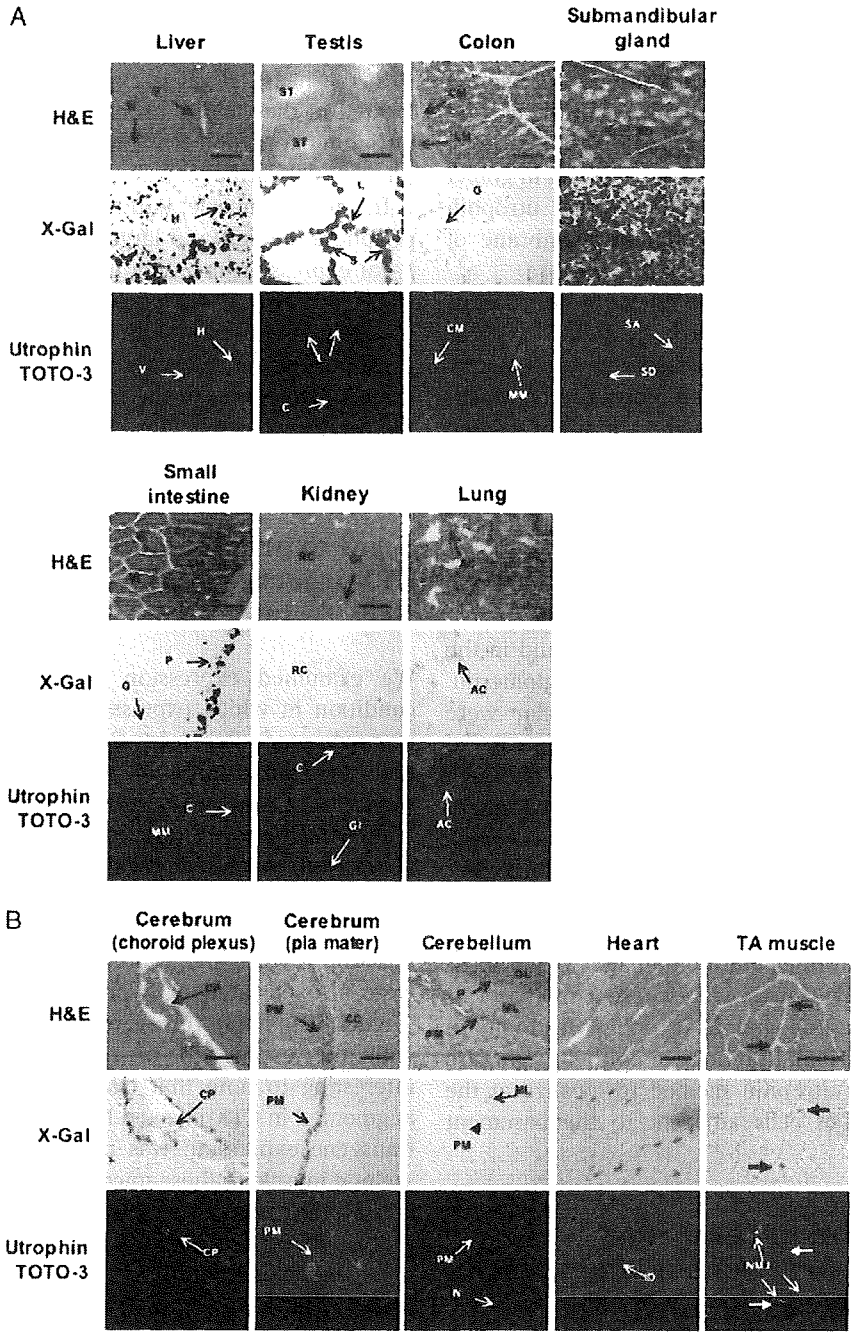

Figure 3. Histological and immunohistochemical analysis of DUE Tg mice. Serial cryosections of tissues [liver, testis, colon, submandibular gland, small intestine, kidney, and lung (A), cerebrum, cerebellum, heart, and TA muscle (B)] from 7-week-old DUE line 1 Tg mice were stained with H&E (top), X-Gal (middle), and a polyclonal antibody against utophin (UT-2; green) (bottom). Nuclei were stained with TOTO-3 (blue). The NMJs were identified with α-BTX (red) in TA muscle. V, terminal hepatic venule; Si, sinusoid; H, hepatocyte; ST, seminiferous tubule; L, Leydig cell; S, Sertoli cell; C, capillary; CM, inner circular muscle layer; G, goblet cell; LM, outer longitudinal muscle layer; MM, muscularis mucosa; SD, striated duct; Sc, serous secretory cell; SA, serous acinus; Vi, villus; Cr, crypt; P, Paneth cell; C, capillary; RC, renal cortex; Gl, glomerulus; AC, alveolar cells; CP, choroid plexus; PM, pia mater; CC, cerebral cortex; N, neuron; ML, molecular layer; GL, granular layer; P, Purkinje cell; ID, intercalated disk; NMJ, neuromuscular junction. Scale bar = 100 μm

compared with β-gal expression in Gnls Tg mice, the expression levels of the transgene in DUE Tg mice were similar in the liver, testis, colon, submandibular gland, and small intestine, but were elevated in the kidney and lung. In addition, when transgene expression was examined at the protein level, the levels were higher in DUE line 1 Tg mice than those in line 2 Tg mice.

In the liver, the nuclei of hepatocytes, but not sinusoid lining cells, were strongly stained with X-gal, whereas endogenous utrophin was detected in the margins of hepatocytes along sinusoids and terminal hepatic venules.

In the testis, β-gal activity was found in Sertoli cells in the basal compartment of the seminiferous tubules, but not in the adluminal compartment, and in Leydig

cells in the interstitial supporting tissues between the seminiferous tubules. Consistent with this observation, endogenous utrophin signals were found along the basement membrane of the seminiferous tubules and Leydig cells.

In the colon, β-gal-positive nuclei were found in goblet cells in large intestinal glands. Endogenous utrophin signals were found along the basement membrane of large intestinal glands and the muscularis mucosa.

In the submandibular gland, the nuclei of both serous and mucous secretory cells were clearly stained with X-gal. The striated duct epithelia lacked the β-gal signal. Endogenous utrophin was detected along the basement membrane of serous and mucous acini, but not of striated ducts.

In the small intestine, β-gal-positive nuclei were found in goblet cells and Paneth cells, which lie in epithelia of the bases of villi and crypts. Endogenous utrophin signals were found along the basement membrane of villi and crypts and in the muscularis mucosa.

In the kidney, β-gal-positive nuclei were found in the epithelia of cortical renal tubules, but not in glomeruli. It is not clear whether β-gal positive nuclei were present in proximal convoluted tubules, distal convoluted tubules, collecting tubules, or collecting ducts, although endogenous utrophin was found along the basement membrane of cortical renal tubules, collecting ducts of the renal medulla and Bowman's capsules, and in glomerular capillaries.

In the lung, β-gal-positive nuclei were found in alveoli, but not in terminal bronchiole epithelia. It is not clear whether β-gal-positive nuclei were present in type I or type II pneumocytes. Endogenous utrophin was found in alveolar cells and terminal bronchiole epithelia. In these tissues, endogenous utrophin seemed to localize at the plasma membranes of cells adjacent to the basement membranes.

β-gal expression in cerebrum, cerebellum, heart, and skeletal muscle of DUE Tg mice

In a previous study of Gnls Tg mice, we did not detect any β-gal expression in the cerebrum, cerebellum, heart, and skeletal muscle [24], but we found β-gal expression in these tissues in the DUE line 1 Tg mice (Figure 3B).

In the cerebrum, β-gal positive nuclei were found in ependymal cells of the choroid plexus and in fibroblastic cells of the pia mater along the basal membrane. Consistent with this observation, endogenous utrophin was detected in the choroid plexus and pia mater.

In the cerebellum, β-gal-positive nuclei were found in stellate and basket cells of the molecular layer, but not in fibroblastic cells of the pia mater, although endogenous utrophin is expressed in the pia mater of the cerebellum. Our results indicate that the distal utrophin enhancer cannot activate expression of the transgene in fibroblastic cells of the pia mater in the cerebellum, although it can enhance the expression in fibroblastic cells of the pia mater in the cerebrum.

In the heart, β-gal is expressed in myocardial nuclei located in the vicinity of intercalated disks. Endogenous utrophin expression was found in intercalated disks and T tubules of cardiac muscle.

In skeletal muscle, A-utrophin is expressed in NMJs, peripheral nerves, and larger blood vessels. We detected β-gal expression not only in myonuclei located close to NMJs, but also in myonuclei remote from NMJs in DUE Tg skeletal muscles, although it is not clear whether β-gal-positive nuclei were present in nerves and blood vessels. Expression of the transgene was not detected in the cerebrum, cerebellum, heart, and skeletal muscle in DUE line 2 Tg mice.

β-gal expression was augmented in CTX-injected and dystrophin-deficient DUE Tg mice

We examined expression of the transgene under a condition in which expression of endogenous utrophin is augmented. Recently, Galvagni *et al.* [10] reported that the transcription of A-utrophin was activated in regenerating muscle under DUE control. Therefore, we injected CTX into TA muscles of Tg mice to damage muscle fibers, and analysed β-gal expression during muscle regeneration (Figure 4). The β-gal signals were strongly detected in extrasynaptic regions at 5 or 7 days after CTX injection (Figure 4A). Moreover, transgene mRNA levels were also elevated at 3 or 5 days after CTX injection (Figure 4B). These transgene expressions coincided well with the expression of endogenous utrophin. It is interesting to note that transgene expression was also augmented in CTX-injected DUE line 2 Tg mice, although transgene expression was not detected in non-injected skeletal muscle of these mice (Figure 4C).

Utrophin was also up-regulated in the dystrophic process of *mdx* mouse skeletal muscle. To examine the transgene expression in dystrophin-deficient muscle, we mated DUE line 2 Tg male mice with *mdx* female mice (Figure 1D). Endogenous utrophin was overexpressed along the sarcolemma, and some myonuclei of TA and GC muscles of DUE line 2 Tg/*mdx* male mice were positive for β-gal (Figure 5A). We also found slightly elevated mRNA levels derived from the transgene in TA and GC muscles of DUE line 2 Tg/*mdx* mice by RT-PCR (Figure 5B).

Transgene expression was activated in late stage muscle differentiation *in vitro*

We cultured primary myoblasts from skeletal muscles of DUE Tg and Gnls Tg mice, and some of the cultures were induced to differentiate. Those cells were stained with X-Gal (Figure 6A). Expression of the transgene was detected in primary myoblasts of DUE Tg mice, but

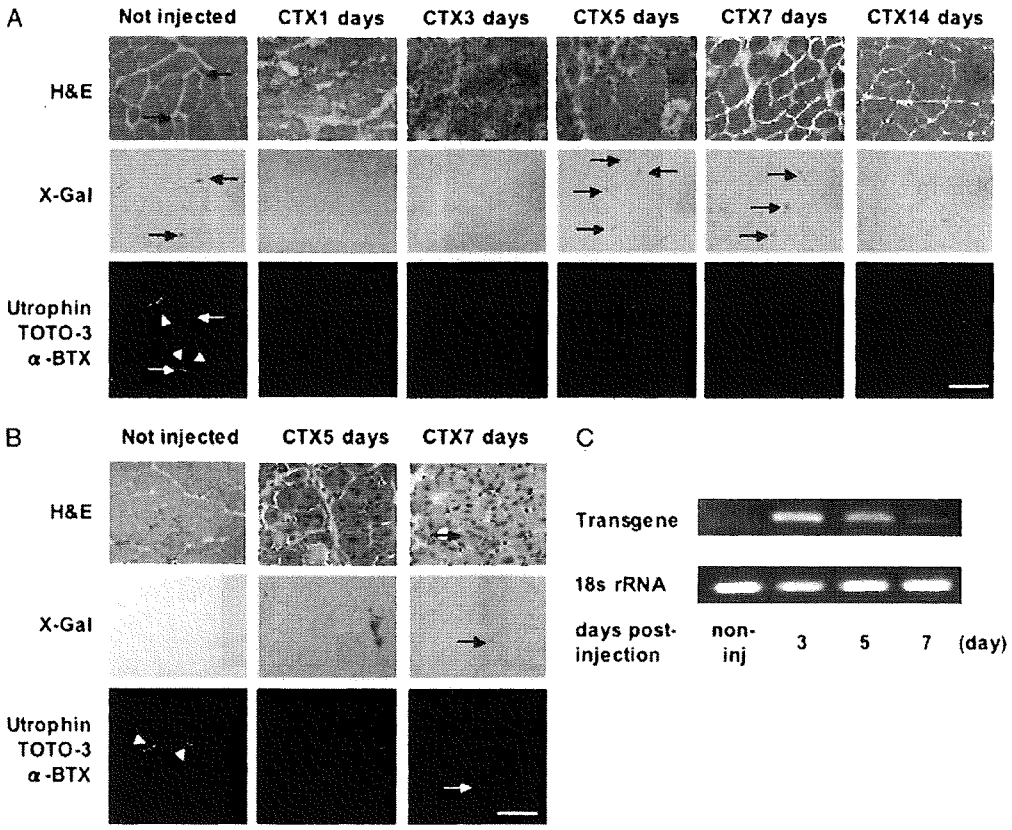

Figure 4. Transgene expression during muscle regeneration in CTX-injected DUE Tg mice. Cryosections of muscles were stained with H&E (top), X-Gal (middle), and a polyclonal antibody against utophin (UT-2; green) (bottom). Nuclei were stained with TOTO-3 (blue). The NMJs were identified with α-BTX (red). (A) TA muscle of DUE line 1 Tg mice at 0, 1, 3, 5, 7, or 14 days after CTX injection. (B) TA muscle of DUE line 2 Tg mice at 0, 5, or 7 days after CTX injection. Arrowhead, NMJ; scale bar = 100 μm. (C) Representative photomicrographs of EtBr-stained agarose gels depicting cDNA products for the transgene and 18s rRNAs from RT-PCR analysis of total RNA from CTX-injected TA muscle of DUE line 1 Tg mice at 0, 3, 5, or 7 days after CTX injection

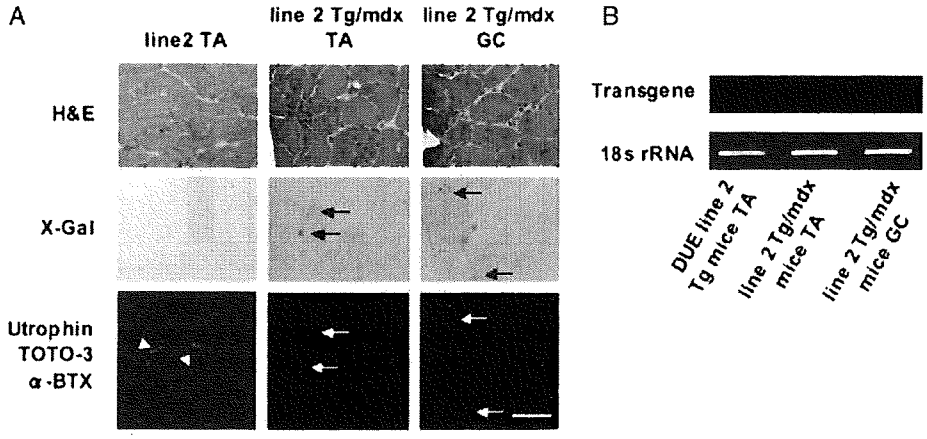

Figure 5. Transgene expression in skeletal muscle of DUE Tg mice cross-bred with dystrophin-deficient mdx mice. (A) Cryosections of muscles were stained with H&E (top), X-Gal (middle), and a polyclonal antibody against utophin (UT-2; green) (bottom). Nuclei were stained with TOTO-3 (blue). The NMJs were identified with α-BTX (red). TA and GC muscles of DUE line 2 Tg/mdx mice. Arrow, β-gal-expressing nuclei; scale bar = 100 μm. (B) Representative photomicrographs of EtBr-stained agarose gels depicting cDNA products for the transgene and 18s rRNAs from RT-PCR analysis of total RNA from TA and GC muscles of DUE line 2 Tg/mdx mice. As a control, the TA muscle of DUE line 2 Tg mice was used

not in those of Gnls Tg mice (Figure 6). In addition, the expression was up-regulated in myotubes in the DUE Tg mice, but not altered in myotubes of the Gnls Tg mice (Figures 6B and 6C). The up-regulation of the transgene was further investigated at the mRNA level, and it was found at a later stage of muscle differentiation. Interestingly, the expression profiles of β-gal and endogenous utrophin were in accordance with that of MEF2C, but not compatible with that of myogenin.

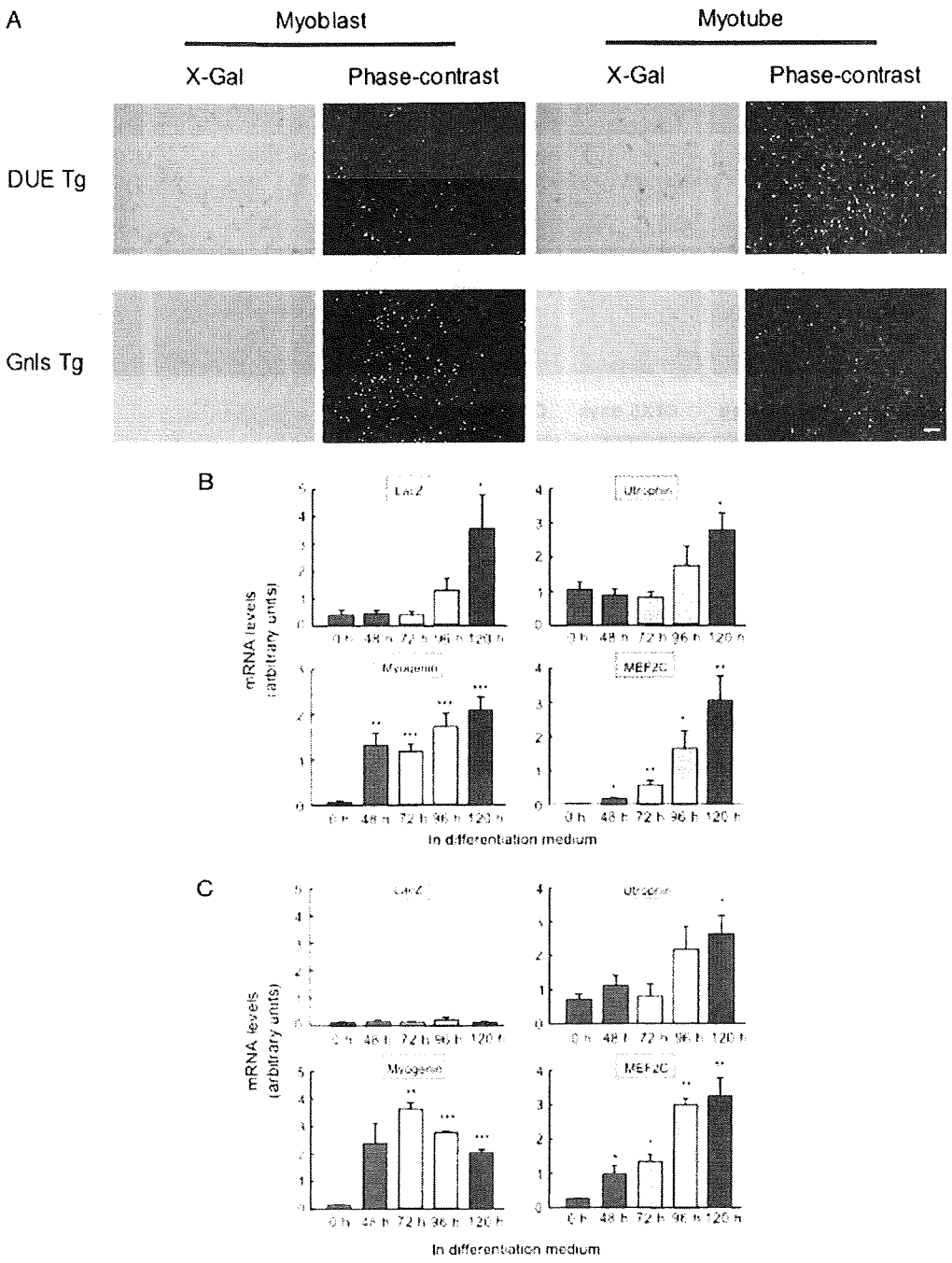

Figure 6. Transgene expression in primary cultured myoblasts and myotubes from DUE Tg mice. (A) Primary cultured myoblasts and myotubes from DUE Tg mice and Gnls Tg mice were stained with X-Gal. Image of myotube after 3 days in differentiation medium. Scale bar = 200 μm. (B, C) Quantification of q-RT-PCR products for transgene, A-utrophin, myogenin, and MEF2C optimized to expression of 18s rRNA in primary myoblasts and myotubes from DUE Tg mice and Gnls Tg mice. The ratios of the transgene, A-utrophin, myogenin, and MEF2C to 18s rRNA are shown as the mean ± SEM of four independent experiments performed in triplicate. $^{*}p < 0.05$, $^{**}p < 0.01$ and $^{***}p < 0.001$ (versus 0 time)

Discussion

We previously showed that a 5385-bp 5′-flanking region of the utrophin gene containing the A-utrophin core promoter drives high levels of transgene expression in liver, testis, colon, submandibular gland, and small intestine, but not in heart and skeletal muscle [24]. In the present study, we demonstrated that addition of DUE to the 5385-bp 5′-flanking region enabled transgene expression in a pattern that was almost identical to that endogenous utrophin expression (Tables 1 and 2). Moreover, β-gal-expressing nuclei were basically located in the vicinity of the endogenous utrophin expression in heart and skeletal muscle.

In regenerating muscle of DUE Tg mice and skeletal muscle of DUE Tg/*mdx* mice, which lack dystrophin, the transgene expression was considerably

Table 1. Cells that express β-gal in Gnls Tg and DUE Tg mice and comparison with endogenous utrophin expression

Tissue	Endogenous utrophin	β-Gal expression		
		Gnls	DUE line 1	DUE line2
Liver	Surface of hepatocyte	Hepatocyte	Hepatocyte	Hepatocyte
Testis	BM of seminiferous tubule	Sertoli cell	Sertoli cell	Sertoli cell
	Leydig cell	Leydig cell	Leydig cell	Leydig cell
Colon	BM of large intestinal gland	Goblet cell	Goblet cell	Goblet cell
	Muscularis mucosa	ND	ND	ND
Submandibular gland	BM of serous & mucous acinus	Serous & mucous secretory cell	Serous & mucous secretory cell	Serous & mucous secretory cell
Small intestine	BM of villus & crypt	Paneth cell, goblet cell	Paneth cell, Goblet cell	Paneth cell, Goblet cell
	Muscularis mucosa	ND	ND	ND
Kidney	BM of cortical renal tubule	Epithelial cell of cortical renal tubule	Epithelial cell of cortical renal tubule	Epithelial cell of cortical renal tubule
	BM of collecting duct in renal medulla			
	Glomerulus	ND	ND	ND
Lung	Alveolus	Alveolar cell	Alveolar cell	Alveolar cell
	Terminal bronchiole epithelium	ND	ND	ND
Cerebrum	Choroid plexus	ND	Ependymal cell of choroid plexus	ND
	Pia mater		Fibroblastic cell of pia mater	
Cerebellum	Pia mater	ND	Stellate cell and basket cell of molecular layer	ND
Heart	Intercalated disk	ND	Peripheral cell of intercalated disk	ND
	T tubule			
Skeletal muscle	Neuromuscular junction	ND	Peripheral cell of neuromuscular junction	ND
	Myotendinous junction			
	Regenerating muscle fiber			

The localization of endogenous utrophin is based on this study and previous studies [11,24]. BM, basement membrane; ND, not detected.

Table 2. Summary of β-gal expression in Gnls Tg mice and DUE Tg mice

	Gnls	DUE line 1	DUE line 2
Liver	++	++	±
Testis	+++	+++	+
Colon	++	++	+
Submandibular gland	+++	+++	+
Small intestine	+	+	±
Kidney	±	+	+
Lung	+	++	±
Cerebrum	-	++	-
Cerebellum	-	++	-
Heart	-	++	-
TA muscle	-	+	-

Tg mice were sacrificed at 4–7 weeks, and β-gal expression was examined in several tissues. No β-gal positive nuclei were found in nontransgenic littermates. β-gal expression levels: −, none; ±, trace; +, weak; ++, moderate; +++, strong.

up-regulated. Another study [10] also reported that utrophin transcription was controlled by DUE activity in regenerating muscle and that its activity was dependent on an AP-1 binding site. Injection of marcain into TA muscles of CD1 mice demonstrated elevation of members of the AP-1 factor, *c-fos, fosB, fra-1, fra-2, c-jun, junB* and *junD* [10]; however, we also found distinct elevation of *c-fos* and *fra-1* mRNA in our regeneration system (unpublished observations).

We cultured primary myogenic cells from DUE Tg mice and found that transgene expression was up-regulated during the differentiation process. Moreover, these transgene expression patterns corresponded to the endogenous utrophin expression profile. This result indicates that the participation of DUE in utrophin expression during muscle regeneration might depend largely on DUE activity in the later stage of muscle differentiation. It is intriguing to note that transgene and endogenous utrophin expression patterns coincided with the expression profile of MEF2C, but not that of myogenin. It has been already reported that MEF2C mediates the promoter activity of c-jun [33]. The MEF2C-c-jun pathway is one of the candidates for regulation of utrophin expression via DUE. Analysis of the transcriptional factors that interact with DUE sequences, particularly the AP-1 site, would be very intriguing and should be clarified by a future study.

In the present study, we also demonstrated that the addition of DUE augmented transgene expression not only in the heart and skeletal muscle, but also in other tissues, such as the cerebral pia mater and choroid plexus and the cerebellar choroid plexus and molecular layer. In addition, transgene expression was elevated in the kidney and lung of DUE Tg mice compared to that of Gnls Tg mice, although it is necessary to consider the difference in transgene copy numbers. These results suggest that DUE activity is not muscle specific, consistent with the data of Galvagni *et al.* [26]. In their study, a construct of DUE added to the utrophin promoter was transiently transfected to various cells and revealed that DUE enhanced utrophin promoter activity not only in C2C12 myoblasts, but also in HeLa cells and RD cells.

However, the addition of DUE cannot fully explain the transcriptional regulation of utrophin. In the cerebrum and cerebellum, endogenous utrophin was expressed in the pia mater and choroid plexus. We found β-gal-positive

nuclei in the cerebral pia mater along the basal lamina, but did not find many β-gal-positive nuclei in the cerebellum. There are several possibilities to explain this discrepancy. The first possibility is that the domain that regulates utrophin expression in the pia mater of the cerebellum is different from that for the pia mater in the cerebrum. The second possibility is that transcription of utrophin might be less active in fibroblastic cells of the pia mater of cerebellum compared to those in the cerebrum. However, a fundamental difference between fibroblastic cells in the cerebrum and those in the cerebellum has not been reported; further experiments are required to explain this discrepancy.

We demonstrated that DUE is necessary for utrophin expression in skeletal muscle, but the increase in the utrophin expression level was much larger than the transgene expression in regenerated muscle. Another study [11] also detected the increase in the abundance of A-utrophin protein in muscle from *mdx* mice but could not find any parallel elevation in the levels of utrophin transcripts. Therefore, A-utrophin expression may also be regulated at the post-transcriptional level. Indeed, recent studies have shown that distinct cis-acting elements within the utrophin 3′-UTR were important not only for controlling the stability of utrophin transcripts in muscle cells, but also for targeting them to specific subcellular locations [34,35].

Post-translational levels are also important for utrophin expression through stabilization of the protein. DAPs such as dystrophin, β-dystroglycan, α-dystroglycan, and α-sarcoglycan have been linked to regulation by protein degradation mechanisms including the ubiquitin-proteasome pathway [36] and calpain-mediated proteolysis [37]. Inhibition of the proteasomal degradation pathway was found to rescue the expression levels of several DAPs in *mdx* mice [36]. Treatment of normal and DMD human myotubes with glucocorticoid induced utrophin protein without elevations in transcripts, and this was suggested to involve calpain inhibition [38].

It is likely that extrasynaptic expression of utrophin in skeletal muscle of DMD patients would ameliorate the dystrophic pathology, at least to some extent [17,18]. The results of the present study demonstrate that DUE is indispensable to utrophin expression in skeletal muscle and heart. To further investigate the up-regulation mechanisms of utrophin in both tissues, we need to search for transcription factors bound to DUE. In addition, we established primary myogenic cell cultures from DUE Tg mice and found that utrophin up-regulation depends on the DUE motif during muscle differentiation. These cells provide a high through-put screening system for drugs that can up-regulate utrophin expression in myogenic cells.

Acknowledgements

We thank Dr Imamura for giving the utrophin antibody. We also thank all members of the Department of Molecular Therapy, National Institute of Neuroscience, for technical assistance and useful discussion and suggestions, especially S. Fukada, A. Uezumi, and M. Ikemoto. This work is supported by grants for Research on Nervous and Mental Disorders (grant 16B-2); Health Science Research Grants for research on the human genome and gene therapy (H16-genome-003) and for research on brain science (H15-kokoro-021 and H18-kokoro-019) from the Japanese Ministry of Health, Labour, and Welfare; Grants-in-Aid for Scientific Research (14657158, 15390281, 16590333, 17590857, and 18590392) from the Japanese Ministry of Education, Culture, Sports, Science, and Technology; and the Ground-based Research Program for Space Utilization, promoted by Japan Space Forum.

References

1. Koenig M, Hoffman EP, Bertelson CJ, *et al.* Complete cloning of the Duchenne muscular dystrophy (DMD) cDNA and preliminary genomic organization of the DMD gene in normal and affected individuals. *Cell* 1987; **50**: 509–517.
2. Ahn AH, Kunkel LM. The structural and functional diversity of dystrophin. *Nat Genet* 1993; **3**: 283–291.
3. Tinsley JM, Blake DJ, Zuellig RA, *et al.* Increasing complexity of the dystrophin-associated protein complex. *Proc Natl Acad Sci USA* 1994; **91**: 8307–8313.
4. Campbell KP. Three muscular dystrophies: loss of cytoskeleton-extracellular matrix linkage. *Cell* 1995; **80**: 675–679.
5. Ozawa E, Yoshida M, Suzuki A, *et al.* Dystrophin-associated proteins in muscular dystrophy. *Hum Mol Genet* 1995; **4**: 1711–1716.
6. Pearce M, Blake DJ, Tinsley JM, *et al.* The utrophin and dystrophin genes share similarities in genomic structure. *Hum Mol Genet* 1993; **2**: 1765–1772.
7. Grady RM, Teng H, Nichol MC, *et al.* Skeletal and cardiac myopathies in mice lacking utrophin and dystrophin: a model for Duchenne muscular dystrophy. *Cell* 1997; **90**: 729–738.
8. Khurana TS, Watkins SC, Chafey P, *et al.* Immunolocalization and developmental expression of dystrophin related protein in skeletal muscle. *Neuromuscul Disord* 1991; **1**: 185–194.
9. Ohlendieck K, Ervasti JM, Matsumura K, *et al.* Dystrophin-related protein is localized to neuromuscular junctions of adult skeletal muscle. *Neuron* 1991; **7**: 499–508.
10. Galvagni F, Cantini M, Oliviero S. The utrophin gene is transcriptionally up-regulated in regenerating muscle. *J Biol Chem* 2002; **277**: 19106–19113.
11. Weir AP, Burton EA, Harrod G, *et al.* A- and B-utrophin have different expression patterns and are differentially up-regulated in mdx muscle. *J Biol Chem* 2002; **277**: 45285–45290.
12. Takemitsu M, Ishiura S, Koga R, *et al.* Dystrophin-related protein in the fetal and denervated skeletal muscles of normal and mdx mice. *Biochem Biophys Res Commun* 1991; **180**: 1179–1186.
13. Matsumura K, Ervasti JM, Ohlendieck K, *et al.* Association of dystrophin-related protein with dystrophin-associated proteins in mdx mouse muscle. *Nature* 1992; **360**: 588–591.
14. Helliwell TR, Man NT, Morris GE, *et al.* The dystrophin-related protein, utrophin, is expressed on the sarcolemma of regenerating human skeletal muscle fibres in dystrophies and inflammatory myopathies. *Neuromuscul Disord* 1992; **2**: 177–184.
15. Nguyen TM, Ellis JM, Love DR, *et al.* Localization of the DMDL gene-encoded dystrophin-related protein using a panel of 19 monoclonal antibodies: presence at neuromuscular junctions, in the sarcolemma of dystrophic skeletal muscle, in vascular and other smooth muscles, and in proliferating brain cell lines. *J Cell Biol* 1991; **115**: 1695–1700.
16. Tinsley JM, Potter AC, Phelps SR, *et al.* Amelioration of the dystrophic phenotype of mdx mice using a truncated utrophin transgene. *Nature* 1996; **384**: 349–353.
17. Deconinck N, Tinsley J, De Backer F, *et al.* Expression of truncated utrophin leads to major functional improvements in dystrophin-deficient muscles of mice. *Nat Med* 1997; **3**: 1216–1221.

18. Tinsley J, Deconinck N, Fisher R, *et al.* Expression of full-length utrophin prevents muscular dystrophy in mdx mice. *Nat Med* 1998; **4**: 1441–1444.
19. Gilbert R, Nalbantoglu J, Petrof BJ, *et al.* Adenovirus-mediated utrophin gene transfer mitigates the dystrophic phenotype of mdx mouse muscles. *Hum Gene Ther* 1999; **10**: 1299–1310.
20. Yamamoto K, Yuasa K, Miyagoe Y, *et al.* Immune response to adenovirus-delivered antigens upregulates utrophin and results in mitigation of muscle pathology in mdx mice. *Hum Gene Ther* 2000; **11**: 669–680.
21. Dennis CL, Tinsley JM, Deconinck AE, *et al.* Molecular and functional analysis of the utrophin promoter. *Nucleic Acids Res* 1996; **24**: 1646–1652.
22. Burton EA, Tinsley JM, Holzfeind PJ, *et al.* A second promoter provides an alternative target for therapeutic up-regulation of utrophin in Duchenne muscular dystrophy. *Proc Natl Acad Sci USA* 1999; **96**: 14025–14030.
23. Jimenez-Mallebrera C, Davies K, Putt W, *et al.* A study of short utrophin isoforms in mice deficient for full-length utrophin. *Mamm Genome* 2003; **14**: 47–60.
24. Takahashi J, Itoh Y, Fujimori K, *et al.* The utrophin promoter A drives high expression of the transgenic LacZ gene in liver, testis, colon, submandibular gland, and small intestine. *J Gene Med* 2005; **7**: 237–248.
25. Hirst RC, McCullagh KJ, Davies KE. Utrophin upregulation in Duchenne muscular dystrophy. *Acta Myol* 2005; **24**: 209–216.
26. Galvagni F, Oliviero S. Utrophin transcription is activated by an intronic enhancer. *J Biol Chem* 2000; **275**: 3168–3172.
27. Kalderon D, Roberts BL, Richardson WD, *et al.* A short amino acid sequence able to specify nuclear location. *Cell* 1984; **39**: 499–509.
28. Ishii A, Hagiwara Y, Saito Y, *et al.* Effective adenovirus-mediated gene expression in adult murine skeletal muscle. *Muscle Nerve* 1999; **22**: 592–599.
29. Imamura M, Ozawa E. Differential expression of dystrophin isoforms and utrophin during dibutyryl-cAMP-induced morphological differentiation of rat brain astrocytes. *Proc Natl Acad Sci USA* 1998; **95**: 6139–6144.
30. Couteaux R, Mira JC, d'Albis A. Regeneration of muscles after cardiotoxin injury. I. Cytological aspects. *Biol Cell* 1988; **62**: 171–182.
31. Rando TA, Blau HM. Primary mouse myoblast purification, characterization, and transplantation for cell-mediated gene therapy. *J Cell Biol* 1994; **125**: 1275–1287.
32. Uezumi A, Ojima K, Fukada S, *et al.* Functional heterogeneity of side population cells in skeletal muscle. *Biochem Biophys Res Commun* 2006; **341**: 864–873.
33. Coso OA, Montaner S, Fromm C, *et al.* Signaling from G protein-coupled receptors to the c-jun promoter involves the MEF2 transcription factor. Evidence for a novel c-jun amino-terminal kinase-independent pathway. *J Biol Chem* 1997; **272**: 20691–20697.
34. Gramolini AO, Belanger G, Jasmin BJ. Distinct regions in the 3′ untranslated region are responsible for targeting and stabilizing utrophin transcripts in skeletal muscle cells. *J Cell Biol* 2001; **154**: 1173–1183.
35. Miura P, Thompson J, Chakkalakal JV, *et al.* The utrophin A 5′-untranslated region confers internal ribosome entry site-mediated translational control during regeneration of skeletal muscle fibers. *J Biol Chem* 2005; **280**: 32997–33005.
36. Bonuccelli G, Sotgia F, Schubert W, *et al.* Proteasome inhibitor (MG-132) treatment of mdx mice rescues the expression and membrane localization of dystrophin and dystrophin-associated proteins. *Am J Pathol* 2003; **163**: 1663–1675.
37. Lescop C, Herzner H, Siendt H, *et al.* Novel cell-penetrating alpha-keto-amide calpain inhibitors as potential treatment for muscular dystrophy. *Bioorg Med Chem Lett* 2005; **15**: 5176–5181.
38. Courdier-Fruh I, Barman L, Briguet A, *et al.* Glucocorticoid-mediated regulation of utrophin levels in human muscle fibers. *Neuromuscul Disord* 2002; **12**: S95–104.

BMC Musculoskeletal Disorders

BioMed Central

Research article

Open Access

Dystrophin deficiency in canine X-linked muscular dystrophy in Japan ($CXMD_J$) alters myosin heavy chain expression profiles in the diaphragm more markedly than in the tibialis cranialis muscle

Katsutoshi Yuasa*[1,2], Akinori Nakamura[2], Takao Hijikata[1] and Shinichi Takeda[2]

Address: [1]Department of Anatomy and Cell Biology, Research Institute of Pharmaceutical Sciences, Faculty of Pharmacy, Musashino University, Nishi-tokyo, Tokyo 202-8585, Japan and [2]Department of Molecular Therapy, National Institute of Neuroscience, National Center of Neurology and Psychiatry, Kodaira, Tokyo 187-8502, Japan

Email: Katsutoshi Yuasa* - k_yuasa@musashino-u.ac.jp; Akinori Nakamura - anakamu@ncnp.go.jp; Takao Hijikata - hijikata@musashino-u.ac.jp; Shinichi Takeda - takeda@ncnp.go.jp

* Corresponding author

Published: 9 January 2008

BMC Musculoskeletal Disorders 2008, 9:1 doi:10.1186/1471-2474-9-1

Received: 28 September 2007
Accepted: 9 January 2008

This article is available from: http://www.biomedcentral.com/1471-2474/9/1

Abstract

Background: Skeletal muscles are composed of heterogeneous collections of muscle fiber types, the arrangement of which contributes to a variety of functional capabilities in many muscle types. Furthermore, skeletal muscles can adapt individual myofibers under various circumstances, such as disease and exercise, by changing fiber types. This study was performed to examine the influence of dystrophin deficiency on fiber type composition of skeletal muscles in canine X-linked muscular dystrophy in Japan ($CXMD_J$), a large animal model for Duchenne muscular dystrophy.

Methods: We used tibialis cranialis (TC) muscles and diaphragms of normal dogs and those with $CXMD_J$ at various ages from 1 month to 3 years old. For classification of fiber types, muscle sections were immunostained with antibodies against fast, slow, or developmental myosin heavy chain (MHC), and the number and size of these fibers were analyzed. In addition, MHC isoforms were detected by gel electrophoresis.

Results: In comparison with TC muscles of $CXMD_J$, the number of fibers expressing slow MHC increased markedly and the number of fibers expressing fast MHC decreased with growth in the affected diaphragm. In populations of muscle fibers expressing fast and/or slow MHC(s) but not developmental MHC of $CXMD_J$ muscles, slow MHC fibers were predominant in number and showed selective enlargement. Especially, in $CXMD_J$ diaphragms, the proportions of slow MHC fibers were significantly larger in populations of myofibers with non-expression of developmental MHC. Analyses of MHC isoforms also indicated a marked increase of type I and decrease of type IIA isoforms in the affected diaphragm at ages over 6 months. In addition, expression of developmental (embryonic and/or neonatal) MHC decreased in the $CXMD_J$ diaphragm in adults, in contrast to continuous high-level expression in affected TC muscle.

Conclusion: The $CXMD_J$ diaphragm showed marked changes in fiber type composition unlike TC muscles, suggesting that the affected diaphragm may be effectively adapted toward dystrophic stress by switching to predominantly slow fibers. Furthermore, the MHC expression profile in the $CXMD_J$ diaphragm was markedly different from that in *mdx* mice, indicating that the dystrophic dog is a more appropriate model than a murine one, to investigate the mechanisms of respiratory failure in DMD.

Background

Duchenne muscular dystrophy (DMD) is an X-linked, lethal disorder of skeletal muscle caused by mutations in the dystrophin gene, which encodes a large sub-sarcolemmal cytoskeletal protein, dystrophin. DMD is characterized by a high incidence (1 in 3,500 boys) and a high frequency of *de novo* mutation [1]. The absence of dystrophin is accompanied by the loss of dystrophin-associated glycoprotein complex from the sarcolemma, leading to reduce membrane stability of myofibers. This dysfunction results in progressive muscle weakness, cardiomyopathy, and subsequent early death by respiratory or heart failure in DMD patients.

For basic and therapeutic studies of DMD, it is very important to perform analysis and evaluation using dystrophin-deficient animal models, such as the *mdx* mouse and dystrophic dog. The *mdx* mouse has been well utilized in many DMD studies, but the murine model shows moderate dystrophic changes unlike severe human DMD [2]. In contrast, golden retriever muscular dystrophy (GRMD) shows similar dystrophic phenotypes to those of human patients: elevated serum CK level, gross muscle atrophy with joint contracture, cardiomyopathy, prominent muscle necrosis, degeneration with mineralization and concurrent regeneration, and endomysial and perimysial fibrosis [3]. Therefore, the dystrophic dog is more suitable than the *mdx* mouse for studies to gain insight into the pathogenic and molecular biological mechanisms of human DMD, as well as for pre-clinical trials [4]. Therefore, we have recently established a colony of beagle-based canine X-linked muscular dystrophy in Japan ($CXMD_J$) [5], and have demonstrated that $CXMD_J$ also exhibited severe symptoms similar to GRMD. To date, we have utilized the littermates of the $CXMD_J$ colony for pathological [6,7], molecular biological [8], and therapeutic examinations [9] of DMD.

Skeletal muscles are composed of heterogeneous populations of muscle fiber types, which contribute to a variety of functional capabilities. In addition, muscle fibers can adapt to diverse situations, such as aging, exercise, and muscular diseases, by changing fiber size or fiber type composition. Therefore, it is important to analyze fiber types to evaluate the condition of skeletal muscle with disease. Fiber types can be distinguished by biochemical, metabolic, morphological, and physiological properties. One of the most informative methods for identification of fiber types is detection of myosin heavy chain (MHC) [10,11]. Myofibers express various MHC isoforms containing slow (type I), fast (types IIA, IIX, IIB), embryonic, and neonatal forms. MHC expression, however, seems to differ between animal species and muscle types. Three MHC isoforms (types I, IIA, and IIX) have been identified in limb skeletal muscles of human and dog, while the fourth isoform, MHC IIB, is abundantly present in small mammals including mouse [10,11]. In addition, expression profiles of MHCs in dystrophin-deficient muscles have been widely examined in limb skeletal muscles of DMD patients [12] and animal models, such as the *mdx* mouse [13] and GRMD [14], but it has not been fully analyzed in skeletal muscles of a canine model. Furthermore, expanded studies of the diaphragm were restricted to that of the *mdx* mouse [13,15]. Therefore, it is important to perform detailed evaluation of fiber types and fiber sizes in limb skeletal muscles and the diaphragm of $CXMD_J$ to understand adaptations toward disease by changes in fiber type composition in the skeletal muscles of human DMD.

In this study, to investigate fiber types of myofibers in dystrophin-deficient skeletal muscles of dystrophic dogs, we evaluated the expression profiles of MHCs in tibialis cranialis (TC) muscles and diaphragms of $CXMD_J$ at various ages, by immunohistochemical and electrophoretic techniques. Briefly, we detected myofibers expressing fast type, slow type, and/or developmental MHCs. In addition, the numbers of fast or slow MHC fibers and the size distribution of these myofibers were analyzed among populations of muscle fibers with or without developmental MHC. The composition of MHC isoforms was also examined in pairs of normal and affected dogs at various ages. This is the first report of evaluation of the detailed distribution of fiber types in TC muscles and diaphragms of dystrophic dogs.

Methods

Animals

Experimental dogs were wild-type and dystrophic littermates at ages from 1 month to 3 years, from the beagle-based $CXMD_J$ breeding colony at National Center of Neurology and Psychiatry (Tokyo, Japan) [5,6]. Within a few days after birth, the genotypes (wild-type, carrier, or dystrophy) of the littermates were determined by a snapback method of single-strand conformation polymorphism (SSCP) analysis [16], and the phenotypes were also confiermed by measuring serum CK level [5]. All animals were cared for and treated in accordance with the guidelines approved by Ethics Committee for Treatment of Laboratory Animals at NCNP, where three fundamental principles (replacement, reduction, and refinement) were also considered. Adult control and $CXMD_J$ dogs (10 months to 3 years) were analyzed in early experiments (three to six animals). Series consisting of a pair of a normal dog and an affected littermate at ages of 1, 2, 4, 6 months, or 1 year old were examined in subsequent experiments. TC muscles and diaphragms were removed from the dogs after necropsy, in which euthanasia was performed by exsanguination under anesthesia with isoflurane taken to prevent unnecessary pain. TC muscle was used as a